

¹⁸⁷Os NMR Study of (η^6 -Arene)osmium(II) Complexes: Separation of Electronic and Steric Ligand Effects†

Andrew G. Bell, Wiktor Koźmiński, Anthony Linden, and
Wolfgang von Philipsborn*‡

Organisch-chemisches Institut, Universität Zürich-Irchel, Winterthurerstrasse 190,
CH-8057 Zürich, Switzerland

Received January 26, 1996[§]

Osmium-187 NMR data have been collected for 37 Os(arene)X₂L type complexes, using inverse two-dimensional (³¹P, ¹⁸⁷Os){¹H} and (¹H, ¹⁸⁷Os) NMR spectroscopy. In the series Os(p-cymene)X₂PMe₃, shielding increases in the order Cl < Br < I < Me < H. Systematic variation of the phosphite ligand of Os(p-cymene)Cl₂P(OR)₃ (R = Me, Et, ⁿBu, Ph, ⁱPr) reveals a linear dependence on Tolman's electronic parameter χ with metal shielding increasing as the acceptor character of the P(OR)₃ ligand increases. Conversely, the structurally related Os(p-cymene)X₂PR₃ types (X = Cl, I; PR₃ = PMe₃, PMe₂Ph, PⁿBu₃, PPh₂Me, P(CH₂Ph)₃, PPh₃, P(m-tolyl)₃, PⁱPr₃, PCy₃) exhibit a linear dependence on Tolman's cone angle θ , with shielding decreasing as larger phosphine ligands are introduced. Variation of the arene ligand of Os(C₆H₅X)Cl₂PMe₃ (X = H, Me, Et, ⁱPr, ^tBu) shows a linear dependence of chemical shift on Taft's steric parameter E_s for group X. In only one case, for the monohydride complexes Os(p-cymene)HClPR₃ (PR₃ = PMe₃, PMe₂Ph, PⁿBu₃, PPh₃, PⁱPr₃, PCy₃), has it been possible to separate both steric and electronic effects of the phosphorus ligand on the observed ¹⁸⁷Os chemical shifts. There are some correlations between ¹J(¹⁸⁷Os,³¹P) and the acceptor character of the phosphorus ligand, and a relationship between Os–P bond lengths and coupling constants was found. Osmium relaxation rates T_1^{-1} and their B_0 field dependence are reported for selected complexes. The crystal structures of four Os(p-cymene)Cl₂L complexes (L = PMe₃ (**1**), P(OMe)₃ (**6**), PBz₃ (**13**), and PPh₃ (**15**)) have been determined.

Introduction

Transition-metal NMR spectroscopy can be used to explore both electronic² and steric³ effects in organometallic systems. In addition, its use as a probe to screen the activity of catalysts,⁴ correlate rate data,⁵ and provide insight into mechanistic pathways⁶ is an ongoing area of research in our group, although these attempts have not always been successful.⁷ Given the current interest in osmium for catalytic transformations,⁸ we decided to examine this nucleus in more detail

as part of our research on the application of transition-metal NMR spectroscopy.

Osmium has two magnetically receptive nuclei, although the ¹⁸⁹Os isotope is not useful because it has a spin of ⁵/₂ and contains a severe quadrupole moment ($Q = 0.91$). The ¹⁸⁷Os isotope has spin ¹/₂ but has a natural abundance of only 1.64% and is the most insensitive nucleus in the periodic table, making its observation by conventional NMR techniques extremely difficult.⁹ For many years, the only known chemical shift was of the reference compound OsO₄.¹⁰ However, the advent of polarization transfer techniques, which require a nonzero scalar $J(M,X)$ coupling, has improved the detection of low- γ spin ¹/₂ nuclei, with sensitivity gains over direct metal detection proportional to (γ_X/γ_M) . Further enhancements are possible by employing indirect 2D spectroscopy, which involves detection of the metal resonance at the frequency of a more receptive spin ¹/₂ nucleus. This gives a factor of $(\gamma_X/\gamma_M)^{5/2}$ increase in sensitivity over direct detection, which for ¹⁸⁷Os NMR spectroscopy corresponds to gains of 1300 and 12 000 for ³¹P and ¹H-detected spectra. These techniques have been applied to other transition-metal nuclei such as ¹⁸³W, ¹⁰³Rh, and ⁵⁷Fe.¹¹

Mann and Maitlis have successfully applied a double INEPT 2D NMR technique to study some μ -hydrido

† Transition Metal NMR Spectroscopy. 32. Part 31: Reference 1.

‡ E-mail: egysi@oci.unizh.ch.

§ Abstract published in *Advance ACS Abstracts*, June 1, 1996.

(1) Meier, E. J. M.; Koźmiński, W.; Lustenberger, P.; Linden, A.; von Philipsborn, W. *Organometallics* **1996**, *15*, 2469.

(2) Graham, P. B.; Rausch, M. D.; Täschler, K.; von Philipsborn, W. *Organometallics* **1991**, *10*, 3049.

(3) (a) Asaro, F.; Costa, G.; Dreos, R.; Pellizer, G.; von Philipsborn, W. *J. Organomet. Chem.* **1996**, *513*, 193. (b) Ludwig, L.; Öhrström, L.; Steinborn, D. *Magn. Reson. Chem.* **1995**, *33*, 984. (c) Elsevier, C. J.; Kowall, B.; Kragten, H. *Inorg. Chem.* **1995**, *34*, 4836. (d) Tavagnacco, C.; Balducci, G.; Costa, G.; Täschler, K.; von Philipsborn, W. *Helv. Chim. Acta* **1990**, *73*, 1469.

(4) (a) Bönemann, H.; Brijoux, W.; Brinkmann, R.; Meurers, W.; Mynott, R.; von Philipsborn, W.; Ego, T. *J. Organomet. Chem.* **1984**, *272*, 231. (b) Bender, B. R.; Koller, M.; Nanz, D.; von Philipsborn, W. *J. Am. Chem. Soc.* **1993**, *115*, 5889.

(5) (a) Koller, M.; von Philipsborn, W. *Organometallics* **1992**, *11*, 467. (b) DeShong, P.; Sidler, D. R.; Rybczynski, J.; Ogilvie, A. A.; von Philipsborn, W. *J. Org. Chem.* **1989**, *54*, 5432. (c) DeShong, P.; Slough, G. A.; Sidler, D. R.; Rybczynski, J.; von Philipsborn, W.; Kunz, R. W.; Bursten, B. E.; Clayton, T. W. *Organometallics* **1989**, *8*, 1381.

(6) Tedesco, V.; von Philipsborn, W. *Organometallics* **1995**, *14*, 3600.

(7) Dowler, M. E.; Le, T.-X.; DeShong, P.; von Philipsborn, W.; Vöhler, M.; Rentsch, D. *Tetrahedron* **1993**, *49*, 5673.

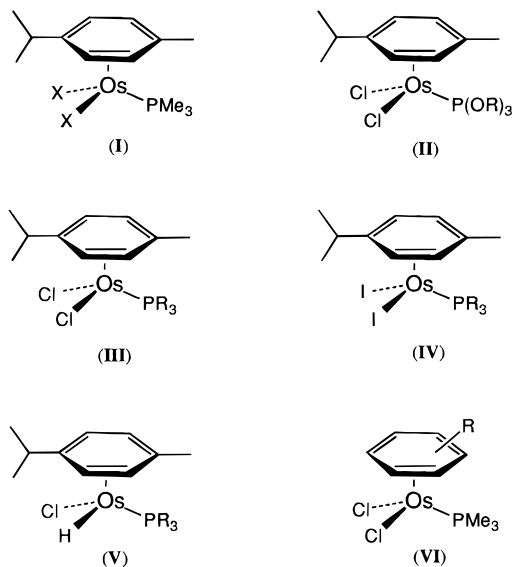
(8) For a recent review of homogeneous catalysis by osmium complexes, see: Sánchez-Delgado, R. A.; Rosales, M.; Esteruelas, M. A.; Oro, A. *J. Mol. Catal. A* **1995**, *96*, 231.

(9) Mason, J., Ed. *Multinuclear NMR*; Plenum Press: New York, 1987.

(10) Kaufmann, J.; Schwenk, A. *Phys. Lett.* **1967**, *24A*, 115.

(11) (a) Pregosin, P. S., Ed. *Transition Metal Nuclear Magnetic Resonance*; Elsevier: Amsterdam, 1991. (b) Mann, B. E. In *Annual Report on NMR Spectroscopy*; Webb, G. A., Ed.; Academic Press: London, 1991; Vol. 23, p 141. (c) von Philipsborn, W. *Pure Appl. Chem.* **1986**, *58*, 513.

Chart 1. Types of Os(arene) X_2 L Complexes Investigated



binuclear osmium complexes.¹² However, the first systematic approach to gaining some $\delta(^{187}\text{Os})$, $J(\text{Os}, X)$, and $T_1(^{187}\text{Os})$ parameters was made more recently by Benn and co-workers for a range of Os(Cp) L_2 R complexes (Cp = η^5 -C₅H₅), using the HMQC technique.¹³ The success of this type of spectroscopy has made it the method of choice for determining $\delta(^{187}\text{Os})$ and $J(\text{Os}, X)$ scalar couplings (X = H, F, P) in later work.^{14,15}

Results and Discussion

An ¹⁸⁷Os NMR study has been made of the six classes of structurally related η^6 -arene-substituted osmium(II) complexes shown in Chart 1.¹⁶ Classes I and VI are PMe_3 substituted but contain various η^1 - and η^6 -ligands, respectively. Classes II and III are dichlorides bearing phosphite and phosphine ligands, class IV compounds are diiodides, and class V compounds are monohydrides. All these types have the advantage of being both soluble, ca. 0.5 M, and stable in CD₂Cl₂ and THF-*d*₈ solvents, allowing for easier detection of the osmium resonance.

X-ray Crystal Structures. Some selected bond angles and lengths for complexes **1**, **6**, **13**, and **15** are given in Table 1, and the crystal structures of **1** (molecule A) and **13** are shown in Figure 1. The structure of **1** has two molecules in the asymmetric unit (A and B); however, there are no major differences in their conformation other than a small rotation of the PMe_3 group. The complexes exhibit a number of structural similarities, as well as some noticeable differences. The PR_3 ligands of **1**, **6**, and **13** adopt a

staggered conformation, with the Os–P bond bisecting the C(2)–C(3) bond of the arene at approximately its midpoint. It is noticeable with **13** that the ⁱPr group bound to the ring points away from the phosphine ligand, as evidenced by the increase in the C(2)–C(1)–C(7)–C(9) torsion angle. However, **15** adopts a conformation in which the Os–P bond bisects the C(4)–C(5) bond distant to the bulky ⁱPr group, presumably for steric reasons, resulting in a restoration of the C(2)–C(1)–C(7)–C(9) torsion angle. The p-cymene ligand is tilted toward the OsCl₂L moiety, placing the C–C bond that bisects the Os–P bond closer to the metal than the parallel C–C bond [C(5)–C(6) or C(1)–C(2)], but this becomes less marked as larger ligands are introduced.

The p-cymene ring is puckered in a manner dictated by the size of the phosphorus ligand. Thus, the χ^2 distributions¹⁷ for deviations of the η^6 -arene atoms C(1) to C(6) from planarity are 30.3 for **1b**, increasing to 289.5 for **15**. For complexes **1** and **13**, atoms C(1) and C(4) lie above the average plane of the η^6 -arene ring, with the others below. However, for the P(OMe)₃-substituted case **6**, the reverse is true. Complex **15** behaves like **6**, except that, due to the change in conformation of the PPh₃ ligand, it is now the C(3)–C(6) axis which lies beneath the plane of the arene ligand. Finally, the crystal structures suggest that as the phosphorus ligand becomes more sterically demanding, the Os–P bond distance increases in length. However, the effect of the ligand on the Os–Cl bond lengths and Cl–Os–Cl bond angles varies, especially for **1**.

Chemical Shifts. Ramsey¹⁸ described nuclear shielding (σ) as arising from a diamagnetic (σ_d) and paramagnetic (σ_p) contribution, of which the former remains fairly constant for a given nucleus. Later work by Griffith and Orgel¹⁹ has elaborated upon the Ramsey model to give a better description for transition metal nuclei, for which the σ_p contribution to the nuclear shielding term is shown in eq 1, where ΔE is the average

$$\sigma_p = -\text{constant} (\Delta E)^{-1} \langle r_d^{-3} \rangle \sum Q_N \quad (1)$$

d–d excitation energy and r_d is the effective radius of the d-orbital electron. The $\sum Q_N$ term describes the distribution of charge in the valence p and d orbitals, which can be assumed to remain fairly constant for structurally related molecules.

Initially, the concentration and temperature dependence of $\delta(^{187}\text{Os})$ was investigated. At 300 K, the shifts of **6** in CD₂Cl₂ exhibit a linear concentration dependence (six points, concentration coefficient 18.3 ppm·L·mol⁻¹), with the osmium resonance at 7.7×10^{-2} M (20 mg in 0.5 mL of solvent) being more highly shielded by 7 ppm than in a 4.6×10^{-1} M solution (120 mg in 0.5 mL). Similarly, a linear temperature coefficient of +0.7 ppm K⁻¹ was observed for a 4.6×10^{-1} M solution of **6** between 233 and 303 K (six points) in polar CD₃CN and nonpolar CD₂Cl₂ solvents. This effect is in the same order as that observed for Fe(CO)₅²⁰ but is substantially less than the value of 2.48 ppm K⁻¹

(12) (a) Cabeza, J. A.; Mann, B. E.; Maitlis, P. M.; Brevard, C. J. *Chem. Soc., Dalton Trans.* **1988**, 629. (b) Cabeza, J. A.; Nutton, A.; Mann, B. E.; Brevard, C.; Maitlis, P. M. *Inorg. Chim. Acta* **1986**, *115*, L47. (c) Cabeza, J. A.; Mann, B. E.; Brevard, C.; Maitlis, P. M. *J. Chem. Soc., Chem. Commun.* **1985**, 65.

(13) (a) Benn, R.; Brenneke, H.; Jousen, E.; Lehmkuhl, H.; Ortiz, F. L. *Organometallics* **1990**, *9*, 756. (b) Benn, R.; Jousen, E.; Lehmkuhl, H.; Ortiz, F. L.; Rufinska, A. *J. Am. Chem. Soc.* **1989**, *111*, 8754.

(14) Christe, K. O.; Dixon, D. A.; Mack, H. G.; Oberhammer, H.; Pagelot, A.; Sanders, J. C. P.; Schrobilgen, G. J. *J. Am. Chem. Soc.* **1993**, *115*, 11279.

(15) Michelman, R. I.; Ball, G. E.; Bergman, R. G.; Andersen, R. A. *Organometallics* **1994**, *13*, 869.

(16) For a review of the organometallic chemistry of (η^6 -arene)Os complexes, see: LeBozec, H.; Touchard, D.; Dixneuf, P. H. *Adv. Organomet. Chem.* **1989**, *29*, 163.

(17) Stout, G. H.; Jensen, L. H. *X-Ray Structure Determination-A Practical Guide*, 2nd ed.; John Wiley & Sons: New York, 1989; p 409.

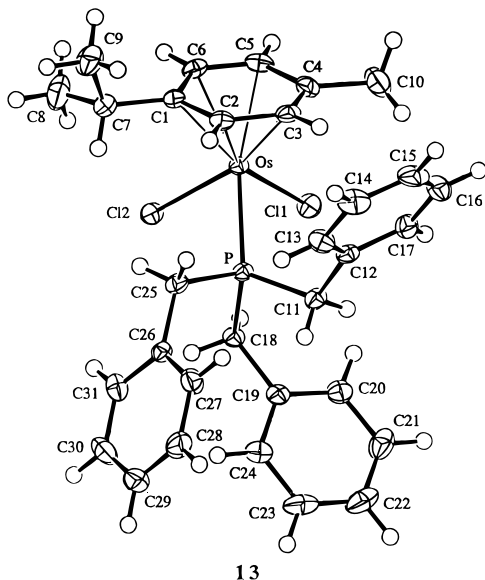
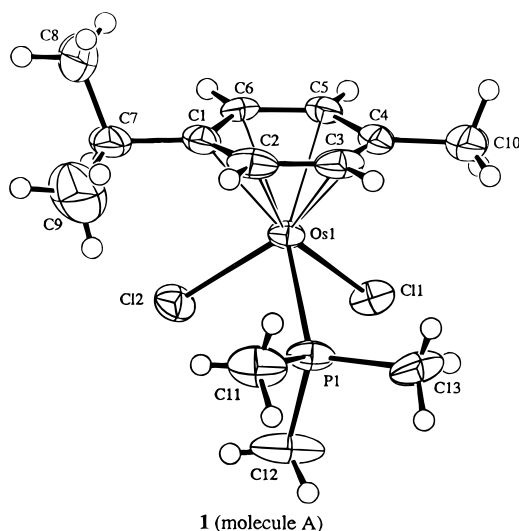
(18) Ramsey, N. F. *Phys. Rev.* **1950**, *77*, 567; *78*, 699; **1951**, *83*, 540; **1952**, *86*, 243.

(19) Griffith, J. S.; Orgel, L. E. *Trans. Faraday Soc.* **1957**, *53*, 601.

(20) Schwenk, A. *Phys. Lett.* **1970**, *31A*, 513.

Table 1. Selected Bond Lengths (Å), Angles (deg), and Torsion Angles (deg) for Complexes **1**, **6**, **13**, and **15**

	1				
	molecule A	molecule B	6	13	15
Os–Cl(1)	2.424(2)	2.428(2)	2.422(2)	2.4251(7)	2.427(1)
Os–Cl(2)	2.426(6)	2.416(1)	2.425(2)	2.4220(7)	2.414(1)
Os–P	2.341(2)	2.340(2)	2.281(1)	2.3608(7)	2.355(1)
Os–C(1)	2.201(6)	2.215(6)	2.204(6)	2.212(3)	2.258(4)
Os–C(2)	2.181(6)	2.194(5)	2.180(5)	2.171(3)	2.231(4)
Os–C(3)	2.158(6)	2.186(5)	2.199(6)	2.210(3)	2.187(4)
Os–C(4)	2.184(6)	2.201(5)	2.229(5)	2.225(3)	2.236(4)
Os–C(5)	2.235(5)	2.189(5)	2.270(5)	2.248(3)	2.203(4)
Os–C(6)	2.248(5)	2.236(5)	2.276(5)	2.237(3)	2.169(4)
χ^2 ^a	100.5	30.3	145.4	154.7	289.5
Cl(1)–Os–Cl(2)	85.73(6)	88.00(6)	86.27(6)	87.78(3)	87.18(4)
Cl(1)–Os–P	83.22(6)	82.71(5)	86.37(5)	85.06(3)	85.54(3)
Cl(2)–Os–P	87.94(6)	85.33(6)	90.48(6)	79.69(2)	87.55(4)
C(2)–C(1)–C(7)–C(8)	105.1(9)	110.8(7)	93.7(7)	–168.6(3)	95.1(4)
C(2)–C(1)–C(7)–C(9)	–17.5(9)	–14.5(8)	–31.6(9)	68.0(3)	–29.3(5)

^a Deviation of C(1)–C(2)–C(3)–C(4)–C(5)–C(6) from planarity.¹⁷**Figure 1.** ORTEP⁵⁰ plot of Os(p-cymene)Cl₂PMe₃ (**1**, molecule A) and Os(p-cymene)Cl₂P(CH₂Ph)₃ (**13**) (50% probability ellipsoids; H atoms given arbitrary thermal parameters for clarity).

observed for the complex Fe(Cp)(PPh₃)(CO)(COMe).²¹ Therefore, with careful temperature and concentration

control of our samples, we predict that our chemical shifts are accurate to within ± 1 ppm.

The ¹⁸⁷Os shifts of compounds **1–37** span a range of approximately 3500 ppm in total but show considerable variations according to class (Tables 2–4). The greatest variation (approximately 3000 ppm) occurs in class **I** as the electronegativity of X is varied. Changing alkyl substituents on the η^6 -ligand of **VI** still has a considerable influence on chemical shift (approximately 600 ppm). The phosphine-substituted examples **III** and **IV** exhibit a similar chemical shift range (approximately 550 ppm) while the phosphites **II** and monohydrides **V** contain less variation (approximately 150 ppm). By systematically varying the stereoelectronic properties of the ligands in the coordination sphere of the metal, we have been able to establish a number of structural correlations as a function of the osmium chemical shift and have been able to separate electronic and steric effects.

I. Electronic Effects. Complexes **I** exhibit a “normal” halogen dependence, with deshielding in the order Cl > Br > I > sp³ C > H. Thus, replacement of both chlorine ligands of **1** with bromine results in a 270 ppm shielding of the osmium nucleus (moves to lower frequency). Further displacement of bromine by iodine causes an additional 760 ppm shielding, while the dihydride **5** resonates a further 2000 ppm to lower frequency of the diiodide **4** and is the most shielded example in this study. This indicates that the observed shielding effects are largely determined by the $\langle r_d^{-3} \rangle$ term in eq 1.²² These ligand effects largely parallel those reported by Benn et al.^{13a} for Os(C₅H₅)(PR₃)₂X complexes.

The shifts of complexes **II** (Figure 2) exhibit a good linear relationship ($r = 0.96$) with Tolman’s electronic parameter χ for the P(OR)₃ ligand,²³ with the metal nucleus becoming progressively more shielded with increasing π -acidity (larger χ values). However, with the exception of the P(OMe)₃ complex **6**, type **II** phosphite complexes are more shielded relative to their phosphine counterparts of series **III**. This “inverse”

(21) Meier, E. J. M.; von Philipsborn, W. Unpublished results.

(22) Mason, J. *Chem. Rev.* **1987**, *87*, 1299.(23) Bartik, T.; Himmler, T.; Schulte, H. G.; Seevogel, K. *J. Organomet. Chem.* **1984**, *272*, 29.

Table 2. ^{187}Os and ^{31}P NMR Data (CD_2Cl_2 , 300 K) for Type I and II Complexes

no.	compd	$\delta(^{187}\text{Os})/\text{ppm}$	$\delta(^{31}\text{P})/\text{ppm}$	$^1J(\text{Os,P})/\text{Hz}$	$^nJ(\text{Os,H})/\text{Hz}$
Type I					
1	$\text{Os}(\text{p-cymene})\text{Cl}_2\text{PMe}_3^a$	-2226	-39.2	272	
2	$\text{Os}(\text{p-cymene})\text{Br}_2\text{PMe}_3$	-2495	-48.3	269	
3	$\text{Os}(\text{p-cymene})\text{I}_2\text{PMe}_3$	-3260	-61.6	266	
4	$\text{Os}(\text{p-cymene})\text{ClMePMe}_3$	-3330	-41.8	280	5 (2J)
5	$\text{Os}(\text{p-cymene})\text{H}_2\text{PMe}_3^b$	-5265 ^a	-44.5 ^a	264	79 (1J)
Type II					
6	$\text{Os}(\text{p-cymene})\text{Cl}_2\text{P}(\text{OMe})_3$	-2168	73.6	453	
7	$\text{Os}(\text{p-cymene})\text{Cl}_2\text{P}(\text{OEt})_3$	-2142	69.2	448	
8	$\text{Os}(\text{p-cymene})\text{Cl}_2\text{P}(\text{O}^i\text{Bu})_3$	-2153	68.0	447	
9	$\text{Os}(\text{p-cymene})\text{Cl}_2\text{P}(\text{OPh})_3$	-2257	58.4	477	
10	$\text{Os}(\text{p-cymene})\text{Cl}_2\text{P}(\text{O}^i\text{Pr})_3$	-2076	63.6	442	

^a p-cymene = p-MeC₆H₄CHMe₂. ^b Measured in THF-*d*₈.**Table 3.** ^{187}Os and ^{31}P NMR Data (CD_2Cl_2 , 300 K) of Type III–V Complexes

no.	compd	$\delta(^{187}\text{Os})/\text{ppm}$	$\delta(^{31}\text{P})/\text{ppm}$	$^1J(\text{Os,P})/\text{Hz}$	$^1J(\text{Os,H})/\text{Hz}$
Type III					
1	$\text{Os}(\text{p-cymene})\text{Cl}_2\text{PMe}_3$	-2226	-39.2	272	
11	$\text{Os}(\text{p-cymene})\text{Cl}_2\text{PMe}_2\text{Ph}$	-2162	-33.9	271	
12	$\text{Os}(\text{p-cymene})\text{Cl}_2\text{PPh}_2\text{Me}$	-2097	-20.3	275	
13	$\text{Os}(\text{p-cymene})\text{Cl}_2\text{P}(\text{CH}_2\text{Ph})_3$	-2028	-22.0	278	
14	$\text{Os}(\text{p-cymene})\text{Cl}_2\text{P}^n\text{Bu}_3$	-2081	-26.6	270	
15	$\text{Os}(\text{p-cymene})\text{Cl}_2\text{PPh}_3$	-1906	-13.1	282	
16	$\text{Os}(\text{p-cymene})\text{Cl}_2\text{P}(\text{m-tolyl})_3$	-1892	-14.3	281	
17	$\text{Os}(\text{p-cymene})\text{Cl}_2\text{P}^i\text{Pr}_3$	-1735	-8.5	269	
18	$\text{Os}(\text{p-cymene})\text{Cl}_2\text{PCy}_3$	-1697	-18.7	266	
Type IV					
19	$\text{Os}(\text{p-cymene})\text{I}_2\text{PMe}_2\text{Ph}$	-3201	-54.6	268	
20	$\text{Os}(\text{p-cymene})\text{I}_2\text{PnBu}_3$	-3119	-46.1	268	
21	$\text{Os}(\text{p-cymene})\text{I}_2\text{PPh}_2\text{Me}$	-3173	-37.6	275	
22	$\text{Os}(\text{p-cymene})\text{I}_2\text{PPh}_3$	-3036	-23.7	285	
23	$\text{Os}(\text{p-cymene})\text{I}_2\text{P}^i\text{Pr}_3$	-2738	-21.7	270	
24	$\text{Os}(\text{p-cymene})\text{I}_2\text{PCy}_3$	-2688	-31.2	268	
Type V ^a					
25	$\text{Os}(\text{p-cymene})\text{ClHPMe}_3$	-3758	-40.3	260	73
26	$\text{Os}(\text{p-cymene})\text{ClHPMe}_2\text{Ph}$	-3723	-27.8	264	72.5
27	$\text{Os}(\text{p-cymene})\text{ClHP}^n\text{Bu}_3$	-3814	-9.1	263	72
28	$\text{Os}(\text{p-cymene})\text{ClHPPPh}_2\text{Me}$	-3740	-7.8	270	71
29	$\text{Os}(\text{p-cymene})\text{ClHPPPh}_3$	-3680	-8.2	277	70
30	$\text{Os}(\text{p-cymene})\text{ClHP}^i\text{Pr}_3$	-3764	22.5	265	69
31	$\text{Os}(\text{p-cymene})\text{ClHPCy}_3$	-3738	14.5	264	68.5

^a Measured in THF-*d*₈.**Table 4.** ^{187}Os and ^{31}P NMR Data (CD_2Cl_2 , 300 K) for Type VI Complexes

no.	compd	$\delta(^{187}\text{Os})/\text{ppm}$	$\delta(^{31}\text{P})/\text{ppm}$	$^1J(\text{Os,P})/\text{Hz}$
32	$\text{Os}(\text{C}_6\text{H}_6)\text{Cl}_2\text{PMe}_3$	-2431	-37.5	266
33	$\text{Os}(\text{C}_6\text{H}_5\text{-Me})\text{Cl}_2\text{PMe}_3$	-2364	-37.7	269
34	$\text{Os}(\text{C}_6\text{H}_5\text{-Et})\text{Cl}_2\text{PMe}_3$	-2352	-38.0	270
35	$\text{Os}(\text{C}_6\text{H}_5\text{-}^i\text{Pr})\text{Cl}_2\text{PMe}_3$	-2348	-38.2	270
36	$\text{Os}(\text{C}_6\text{H}_5\text{-}^t\text{Bu})\text{Cl}_2\text{PMe}_3$	-2268	-38.0	267
1	$\text{Os}(\text{p-cymene})\text{Cl}_2\text{PMe}_3$	-2226	-39.2	272
37	$\text{Os}(\text{C}_6\text{Me}_6)\text{Cl}_2\text{PMe}_3$	-1829	-42.3	290

ligand behavior is probably due to an increase in the spectrochemical ΔE parameter caused by a larger metal–ligand orbital interaction of more strongly π -accepting $\text{P}(\text{OR})_3$ ligands. This offsets the deshielding effect expected by way of the associated decrease in the nephelauxetic r_d parameter. An analogous effect was reported for the osmium bis(phosphine) and bis(phosphite) complexes.^{13a}

II. Steric Effects. The shifts of the phosphine-substituted compounds **III** are linearly dependent on Tolman's steric parameter θ for the PR_3 ligand²⁴ ($r = 0.98$) with the osmium nucleus becoming progressively more deshielded as larger phosphine ligands are intro-

duced (Figure 3). Similarly, the iodides **IV**, which are on average 1050 ppm more shielded than **III**, give a linear correlation between $\delta(^{187}\text{Os})$ and θ ($r = 0.97$). There appears to be a mild ligand effect, as the correlation is less significant than for the analogous dichloride complexes **III**. This effect has been observed for some $(\text{Cp}^*)\text{RhX}_2\text{PR}_3$ complexes ($\text{X} = \text{Cl}, \text{Br}, \text{I}$, $\text{Cp}^* = \eta^5\text{-C}_5\text{Me}_5$).²⁵ However, a plot of the osmium shifts of **III** against **IV** is linear ($r = 0.98$), suggesting that the introduction of progressively larger PR_3 ligands in both cases has the same and co-operative effect of decreasing both the ΔE and r_d parameters because of their size.²⁶ Similar observations have been made by Elsevier for some $(\eta^4\text{-COD})\text{Rh}(\text{PR}_3)\text{Cl}$ complexes.^{3c}

The osmium shifts of complexes **VI** reveal a deshielding influence as more sterically demanding arene groups are introduced. Thus, the hexamethylbenzene-substituted complex **37** resonates 600 ppm to higher frequency relative to the parent complex **32**. Unfortunately, relatively little is known about the steric or electronic properties of arene ligands. In steric terms, Maitlis has calculated cone angles of 162 and 192° for the $\text{Ru-C}_6\text{H}_6$

(25) Tedesco, V., von Philipsborn W. *Magn. Reson. Chem.* **1996**, *34*, 373.(26) Rehder, D. *Chimia* **1986**, *40*, 186.(24) Tolman, C. A. *Chem. Rev.* **1977**, *77*, 313.

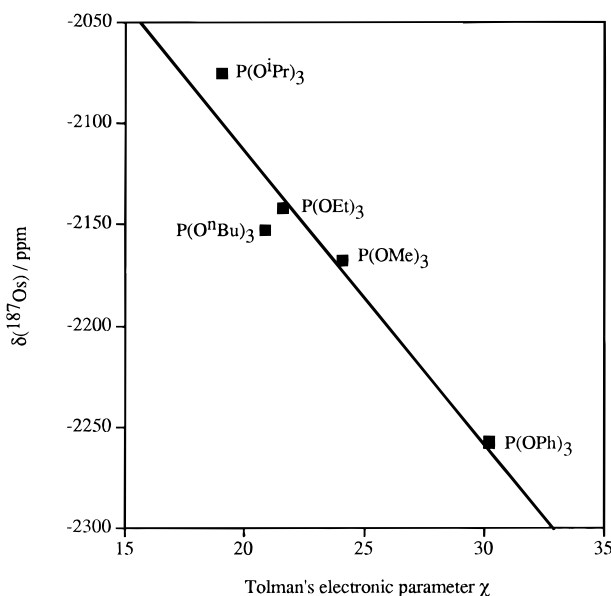


Figure 2. Plot of $\delta(^{187}\text{Os})$ vs Tolman's electronic parameter χ for complexes **II** ($r = 0.96$).

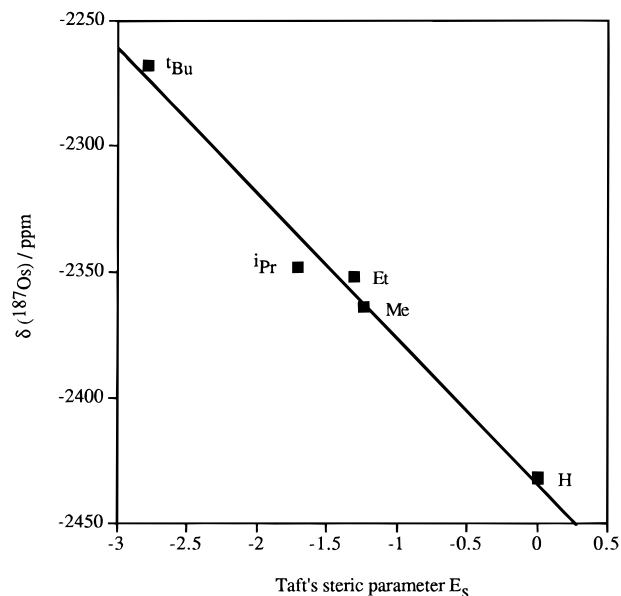


Figure 4. Plot of $\delta(^{187}\text{Os})$ vs Taft's steric parameter E_s for complexes **VI** ($r = 0.99$).

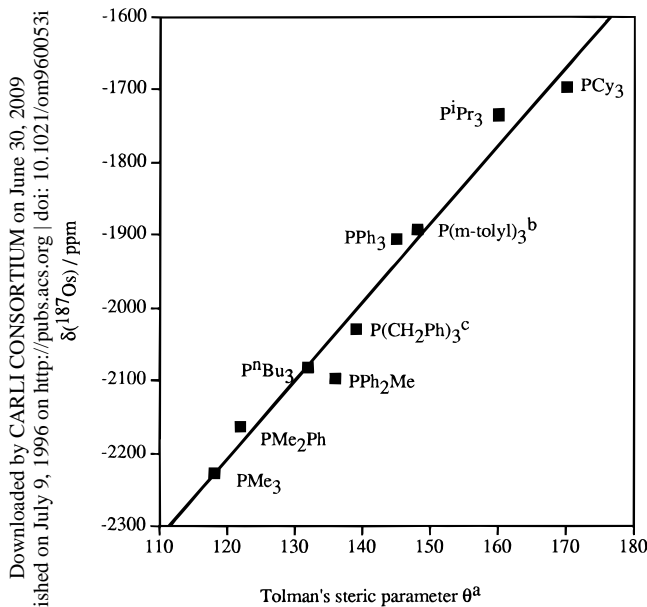


Figure 3. Plot of $\delta(^{187}\text{Os})$ vs Tolman's steric parameter θ for complexes **III** ($r = 0.98$): (a) cone angles taken from ref 24; (b) cone angle taken from ref 34; (c) cone angle determined from crystal structure of **13**.

and Ru-C₆Me₆ moieties.²⁷ Their electronic properties have been more thoroughly investigated by determining core binding energies in the (Cp)Fe(η^6 -arene)⁺ system, using X-ray photoelectron spectroscopy.²⁸ This study has shown that the introduction of a methyl substituent onto the arene slightly enhances its donor properties, although the effect is not great.

We have studied chemical shift correlations with Hammett and Taft-type substituent constants for the five Os(η^6 -C₆H₅X)Cl₂PMe₃ complexes **32–36** (X = H, Me, Et, ⁱPr, ^tBu). Statistically insignificant correlations were obtained for Hammett σ_m , σ_p , σ_p^+ , and σ_p^- and Swain–Lupton F and R values,²⁹ whereas an excellent linear correlation (Figure 4) was obtained using Taft's

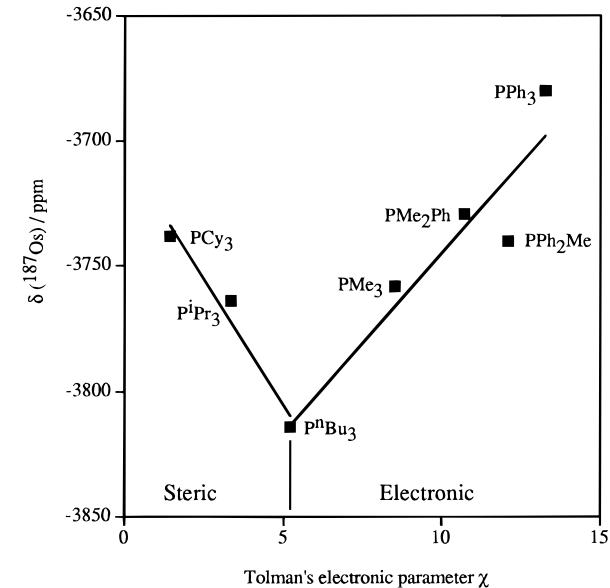


Figure 5. Plot of $\delta(^{187}\text{Os})$ vs Tolman's electronic parameter χ for complexes **V**.

steric parameter E_s ($r = 0.99$).³⁰ This clearly demonstrates the steric origin of the deshielding effects and complements previous observations for ⁵⁹Co,^{3d} ¹⁰³Rh,^{3a,b} and ⁵⁷Fe.¹ The poor correlations obtained using the field and resonance constants, F and R , further suggest that the steric influence of the arene substituent X operates by a combination of field and resonance effects.

III. Mixed Effects. In one case, it has been possible to observe both the electronic and steric effects of similar ligands within the same system. The monohydrides **V** are easily accessible from **III** but give no linear correlation between $\delta(^{187}\text{Os})$ and other structural parameters. A plot of $\delta(^{187}\text{Os})$ against χ (Figure 5) does reveal a near-linear correlation with the ligands PⁿBu₃ to PPh₃, but unlike **II** the metal shifts exhibit a "normal" ligand dependence and are shielded by less π -acidic ligands. This behavior changes when larger and less electroni-

(27) Maitlis, P. M. *Chem. Soc. Rev.* **1981**, 10, 1.

(28) Gassman, P. G.; Deck, P. A. *Organometallics* **1994**, 13, 2890.

(29) Hansch, C.; Leo, A.; Taft, R. W. *Chem. Rev.* **1991**, 91, 165.

(30) March, J. *Advanced Organic Chemistry*, 4th ed.; John Wiley & Sons: New York, 1992; p 285.

cally demanding phosphines (P^iPr_3 and PCy_3) are introduced. These ligands possess virtually no π -acceptor ability and presumably deshield the metal nucleus because of their size, as with **III** and **IV**. Thus, it appears that as the metal becomes more electron rich, the acceptor character of the phosphorus ligand becomes the principal factor determining the chemical shift of the osmium nucleus, with better donor ligands shielding the metal, until a threshold of χ is attained ($\chi < 5.25$, $\theta > 145^\circ$) where steric factors become dominant.

For comparison, we have attempted similar correlations using more conventional ^{31}P NMR methods. For complexes **II** and **III**, χ or θ do not correlate with their absolute ^{31}P shifts but do show modest ($r = 0.93$) and good ($r = 0.98$) correlations, respectively, with their coordination chemical shifts Δ ($\delta_{\text{free ligand}} - \delta_{\text{complex}}$). In contrast, for types **IV–VI** χ or θ do not correlate with either δ or $\Delta(^{31}\text{P})$, thus reflecting a greater sensitivity of the metal nucleus to subtle stereoelectronic changes.

We have been able to use the correlation shown in Figure 3 to determine qualitatively the cone angles of various phosphine ligands by ^{187}Os NMR. For example, literature values for $\text{P}(\text{CH}_2\text{Ph})_3$ ^{24,31} and $\text{P}(\text{m-tolyl})_3$ ³² suggest equivalent cone angles of 165° , which do not correspond with the observed shifts of complexes **13** and **16**. However, these values were measured using simple CPK molecular models with rotation of the R groups to achieve C_{3v} symmetry.³³ Coville has calculated a cone angle of 148° for $\text{P}(\text{m-tolyl})_3$ on the basis of a nonsymmetrical arrangement of the three phenyl rings.³⁴ Evidence for this geometry is now provided by a variable-temperature ^1H NMR investigation of the m-tolyl region of **16** (Figure 6). At room temperature, all three methyl substituents are equivalent, giving a single resonance. However, at -50°C the signal broadens and resolved at -70°C into two separate resonances with a 2:1 ratio, indicating nonequivalence of the m-tolyl groups. Similarly, the crystal structure of complex **13** (Figure 1) reveals a different orientation of the three benzyl groups. One phenyl ring is directed toward the p-cymene group with the other two pointing away, probably to reduce steric interactions about the congested metal center. This arrangement gives a cone angle $5\text{--}6^\circ$ smaller than that measured for the PPh_3 complex **15**.³⁵ These corrected cone angles agree with the observed ^{187}Os shifts obtained for complexes **13** and **16**.

Coupling Constants. A simplified expression to describe one-bond metal–phosphorus coupling constants is given in eq 2,³⁶ where $|\Psi_{\text{M}}(0)|^2$ and $|\Psi_{\text{P}}(0)|^2$

$$J_{\text{M,P}} \propto K\alpha_{\text{M}}^2\alpha_{\text{P}}^2|\Psi_{\text{M}}(0)|^2|\Psi_{\text{P}}(0)|^2\Delta E \quad (2)$$

are s-electron densities at the nucleus of each atom, α^2 represents the localized hybrid bond s-character in a valence bond description, and K is the reduced coupling constant.

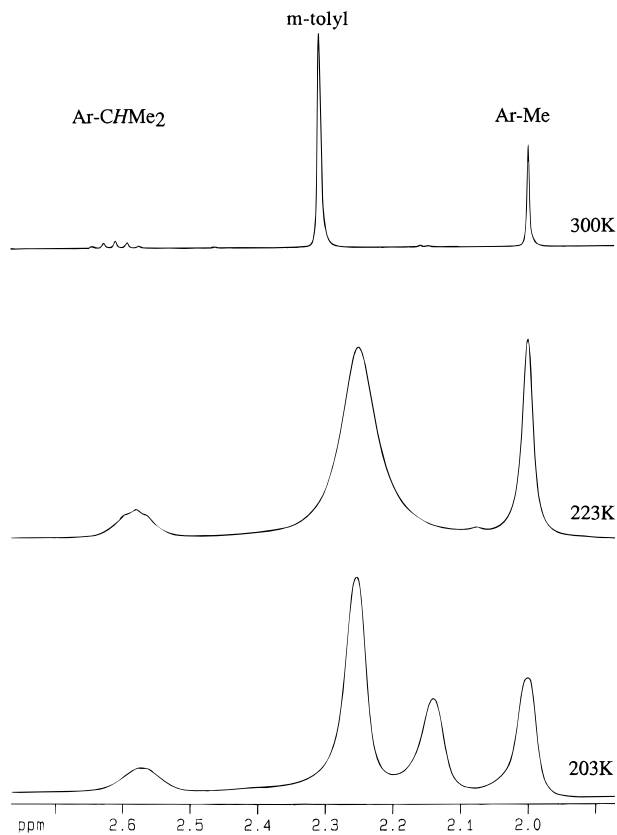


Figure 6. Variable-temperature ^1H -NMR spectra (1.9–2.7 ppm region) of $\text{Os}(\text{p-cymene})\text{Cl}_2\text{P}(\text{m-tolyl})_3$ (**16**) in CD_2Cl_2 at 400 MHz showing two methyl resonances for the $\text{P}(\text{m-tolyl})_3$ ligand at 203 K.

Values of $^1J(\text{M,P})$ scalar coupling constants are known to depend on a number of contributing factors, such as the electronegativity of substituents on phosphorus, metal oxidation state, and structural effects.^{9,36} However, on the basis of the assumption that $^1J(^{187}\text{Os},^{31}\text{P})$ coupling constants are a reflection of the σ -bond order of the M–P bond, we have attempted to correlate these with the spectral properties of the ligands in the metal coordination sphere. The magnitude of $^1J(^{187}\text{Os},^{31}\text{P})$ in series **I** increases in the order $\text{H} < \text{I} < \text{Br} < \text{Cl} < \text{Me}$, but we do not believe that this trend necessarily reflects the Os–P bond strength. It is generally accepted that M–C bonds are weaker than M–H bonds by $15\text{--}25$ kcal mol^{-1} , which may genuinely account for the large $^{187}\text{Os},^{31}\text{P}$ coupling obtained for **4**. However, thermochemical studies of $\text{Ru}(\text{Cp}^*)(\text{PMe}_3)_2\text{X}$ ($\text{X} = \text{Cl}, \text{Br}, \text{I}, \text{H}$) show that the Ru–PMe_3 bond dissociation energy increases in the order $\text{Cl} < \text{Br} \approx \text{I} < \text{H}$.³⁷ A more convincing case is provided by compounds **32–37**, which, with the exception of the ^tBu -substituted complex, show a clear trend of increasing $^1J(^{187}\text{Os},^{31}\text{P})$ with the introduction of larger η^6 -arene ligands. This observation complements the trend observed with $\delta(^{187}\text{Os})$ and clearly suggests a weakening of the osmium–arene bond by larger arene groups, which is also evident from the concomitant strengthening of the Os–P bond.

For types **II** and **III**, $^{187}\text{Os},^{31}\text{P}$ coupling constants are linearly dependent on the electronic character of the phosphorus ligand χ , giving a very modest correlation ($r = 0.86$) for the phosphine series **III**, which improves

(31) Manzer, L. E.; Tolman, C. A. *J. Am. Chem. Soc.* **1975**, *97*, 1955.

(32) (a) Liu, H. Y.; Eriks, K.; Prock, A.; Giering, W. P. *Organometallics* **1990**, *9*, 1758. (b) Rahman, M. M.; Liu, H. Y.; Prock, A.; Giering, W. P. *Organometallics* **1987**, *6*, 650.

(33) Tolman, C. A. *J. Am. Chem. Soc.* **1970**, *92*, 2956.

(34) (a) White, D.; Coville, N. J. *Adv. Organomet. Chem.* **1994**, *36*, 95. (b) White, D.; Carlton, L.; Coville, N. J. *J. Organomet. Chem.* **1992**, *440*, 15.

(35) Cone angles were measured using the equation given in ref 24 with the Os–P bond set to 2.28 Å.

(36) Pregosin, P. S.; Kunz, R. W. *^{31}P and ^{13}C NMR of Transition Metal Phosphine Complexes*; Springer-Verlag: Berlin, 1979.

(37) Bryndza, H. E.; Domaille, P. J.; Paciello, R. A.; Bercaw, J. E. *Organometallics* **1989**, *8*, 379.

Table 5. ^{187}Os Spin–Lattice Relaxation Rates T_1^{-1} (CD_2Cl_2 , 300 K) of Selected Complexes^a

no.	compd	T_1^{-1}/s^{-1}		$T_1^{-1}(\text{csa})$ (%)		T_1^{-1} (other) 9.1 T
		9.4 T	14.1 T	9.4 T	14.1 T	
1	Os(p-cymene) Cl_2PMe_3	0.60	1.3	0.56 (93)	1.4 (100)*	0.04
2	Os(p-cymene) Br_2PMe_3	0.46	0.98	0.42 (91)	0.94 (96)	0.04
3	Os(p-cymene) I_2PMe_3	0.39	0.78	0.31 (79)	0.7 (90)	0.08
6	Os(p-cymene) $\text{Cl}_2\text{P}(\text{OMe})_3$	0.51	1.1	0.47 (92)	1.1 (100)	0.04
7	Os(p-cymene) $\text{Cl}_2\text{P}(\text{OEt})_3$	0.67	1.6	0.74 (100)*	1.7 (100)*	0.0*
8	Os(p-cymene) $\text{Cl}_2\text{P}(\text{O}^n\text{Bu})_3$	0.89	2.0	0.89 (100)	2.0 (100)	0.03
9	Os(p-cymene) $\text{Cl}_2\text{P}(\text{OPh})_3$	0.94	2.2	1.0 (100)*	2.3 (100)*	0.0*
10	Os(p-cymene) $\text{Cl}_2\text{P}(\text{O}^i\text{Pr})_3$	0.71	1.7	0.79 (100)*	1.8 (100)*	0.0*
12	Os(p-cymene) $\text{Cl}_2\text{PPh}_2\text{Me}$	0.88	2.0	0.9 (100)*	2.0 (100)*	0.0*
14	Os(p-cymene) $\text{Cl}_2\text{P}^n\text{Bu}_3$	1.3	3.1	1.4 (100)*	3.2 (100)*	0.0*
15	Os(p-cymene) Cl_2PPh_3	1.2	2.7	1.2 (100)	2.7 (100)	0.0
17	Os(p-cymene) $\text{Cl}_2\text{P}^i\text{Pr}_3$	0.87	2.0	0.9 (100)*	2.0 (100)	0.0*
18	Os(p-cymene) Cl_2PCy_3	1.5	3.3	1.4 (100)	3.2 (100)	0.1

^a Asterisk indicates result of calculation of the CSA relaxation rate greater than 100%, but within limit of experimental error.

greatly ($r = 0.99$) for the phosphites **II**. The magnitude of $^1J(^{187}\text{Os},^{31}\text{P})$ increases with increasing π -acidity of the ligand, which also reflects an increase in the electronegativity of group R. The trialkyl-containing examples of **III** ($\text{R} = \text{Me}, ^n\text{Bu}, ^i\text{Pr}, \text{Cy}, \text{CH}_2\text{Ph}$) exhibit a better correlation against χ with $^1J(^{187}\text{Os},^{31}\text{P})$ generally decreasing with increasing ligand size. However, this behavior deviates considerably when aryl groups are included, as with PPh_2Me , possibly indicating variations in π -bonding interactions for these complexes that are not adequately represented by literature values of χ . Opening of the R–P–R bond angle should increase the phosphorus s character in the P–R bond and decrease χ in the Os–P bond. Thus, larger phosphorus ligands should possess smaller $^{187}\text{Os},^{31}\text{P}$ couplings, but this is not generally observed within a particular series. These results complement the observation made by Nolan for the cleavage of the dimer $[\text{Ru}(\text{p-cymene})\text{Cl}_2]_2$ using various phosphorus ligands. Here, the enthalpy of the reaction was found to increase in the order $\text{PCy}_3 < \text{P}(\text{OPh})_3 < \text{P}^i\text{Pr}_3 < \text{PPh}_3 < \text{P}(\text{CH}_2\text{Ph})_3 < \text{PPh}_2\text{Me} < \text{P}(\text{OMe})_3 < \text{PMe}_2\text{Ph} < \text{PMe}_3$ but with a combination of both electronic and steric factors playing an important role in dictating the magnitude of $-\Delta H$ for the reaction.³⁸

Assuming that the α^2 term in eq 2 makes the dominant contribution to $^1J(^{187}\text{Os},^{31}\text{P})$, the correlations observed against χ for **II** and **III** suggests that larger coupling constants may be a consequence of shorter M–P bond lengths, as has been shown for some platinum complexes.³⁹ We have compared these couplings with our crystallographic data for the phosphines **1**, **13**, and **15** and phosphite **6**. Although the data are not extensive, it does suggest a relationship in our case ($r = 0.96$), although the Os– PMe_3 bond of **1** is slightly shorter than the $^{187}\text{Os},^{31}\text{P}$ coupling would predict. The diiodides **IV** exhibit no similar correlations against χ or θ . This may be an effect of the soft iodine ligand, which can be polarized more easily by the metal to compensate for variations in the bonding requirements of the phosphine.

The monohydrides **V** exhibit no linear correlations between $^1J(^{187}\text{Os},^{31}\text{P})$ and other structural parameters. However, values of $^1J(^{187}\text{Os},^1\text{H})$ were found to give a good correlation with Tolman's steric parameter θ ($r = 0.99$), with coupling constants decreasing with increasing phosphine size. Because infrared measurements of these and related complexes⁴⁰ indicate that the Os–H bond strength increases as larger PR_3 ligands are

introduced, we believe that the correlation is not related to the strength of the Os–H bond. It possibly reflects changes of the H–Os–Cl bond angle to accommodate the ligands across the series PMe_3 ($\theta = 118^\circ$) to PCy_3 ($\theta = 170^\circ$). In conclusion, at least two independent effects (bond distances and angles) can influence the value of one-bond $^{187}\text{Os},^{31}\text{P}$ couplings. Therefore, care has to be taken in any interpretation of this parameter in terms of bond strength.

Relaxation Times. We have been able to measure accurate ^{187}Os T_1 relaxation times for representative examples of types **I–III** (Table 5).⁴¹ Measurements taken of **II** and **III** at 9.4 and 14.1 T show that the rate of relaxation varies from 0.39 to 3.3 s^{-1} and is proportional to the square of the ratio of the two magnetic field strengths (2.25). Hence, the mechanism is chemical shift anisotropy (CSA) dominated. We have compared these T_1 rates with other NMR and structural parameters, but only rough correlations with the molecular weight of the attached phosphorus ligand are apparent, with heavier ligands relaxing the metal nucleus more efficiently than smaller ones within their respective groups. This reflects the molecular tumbling or correlation time, τ_c , of the molecule. However, the phosphites **II** relax at a rate 15–30% slower than their lighter counterparts of **III**, which suggests that other factors are involved. This is also evident in the halogen series $\text{Os}(\text{p-cymene})\text{X}_2\text{PMe}_3$ ($\text{X} = \text{Cl}, \text{Br}, \text{I}$), which shows a trend of slower T_1 rates as the weight of the halogen increases from chlorine to iodine. This is opposed to an effect of τ_c and may be related to the polarization of the Os–X bond, which for more electronegative substituents is greater, thus increasing the anisotropy of the ligand field and of the shielding tensor. Further evidence is provided by the fact that the CSA contribution to T_1 is substantially reduced at the lower field strength. We are currently trying to extend these measurements to more varied types of complexes to determine whether we can extract additional structural information from this NMR parameter.

(38) Serron, S. A.; Nolan, S. P. *Organometallics* **1995**, *14*, 4611.

(39) Mather, G. G.; Pidcock, A.; Rapsey, G. J. N. *J. Chem. Soc., Dalton Trans.* **1973**, 2095.

(40) Bennett, M. A.; Weerasuria, M. M. *J. Organomet. Chem.* **1990**, *394*, 481.

(41) Koźmiński, W.; von Philipsborn, W. *J. Magn. Reson. A* **1995**, *116*, 262.

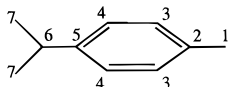
Conclusions

Osmium-187 chemical shifts appear to be very sensitive to subtle changes in the coordination sphere of the metal, making this technique useful in gauging both the electronic and steric effects of various ligands. Some of the electronic ligand effects are similar to those observed in bis(phosphine) complexes of the type $\text{OsCp}(\text{PR}_3)_2\text{X}$ which, however, are characterized by much higher osmium shielding. In addition, osmium-phosphorus and osmium-hydride coupling constants can provide useful structural information in the $\text{Os}(\text{arene})\text{-X}_2\text{L}$ series, in particular on Os-P bond lengths. It is now possible to run ^{187}Os NMR spectra on a routine basis, and we are currently applying the technique to screen the activity of some homogeneous catalysts.

Experimental Section

Inverse-detected ^{187}Os NMR spectra were obtained in CD_2Cl_2 at 300 K using the HMQC technique, with ^{31}P detection at 9.4 T for types **I-IV** and **(VI)** and ^1H detection at 14.1 T for **V**. Approximately 120 mg of sample in 0.5 mL of solvent in a 5-mm NMR tube was required to obtain a phosphorus-detected spectrum using a Bruker AM-400-WB spectrometer equipped with a TBI ^1H , ^{31}P , BB (9–41 MHz) probe head ($\nu_0(^{187}\text{Os}) = 62$ MHz). A second PTS160 synthesizer together with a BSV3 decoupling unit was used for pulsing the osmium frequency. Typically 128 increments, each of 24 scans, were accumulated over 3 h to obtain an overview spectrum: spectral width in F1 30 000 Hz, spectral width in F2 800–1000 Hz, 90° pulse length for osmium 60 μs , 90° phosphorus pulse 14.5 μs , relaxation delay 2 s. Final spectra of 256 increments, each of 40 scans, with a spectral window of 2000 Hz in F1 were measured overnight to ensure that the osmium signals were not folded. Proton-detected spectra were acquired on a Bruker AMX-600 spectrometer, which required only 40 mg of sample, using a TBI-LR ^1H , ^{31}P , BB (7–21.5 MHz) probe head ($\nu_0(^{187}\text{Os}) = 13.8$ MHz). Typically 128 increments, each of 8 or 16 scans, were accumulated in 1 to 2 h: spectral width in F1 800 Hz, spectral width in F2 300 Hz, 90° pulse length for osmium 70–80 μs , 90° for proton 11 μs , relaxation delay 2 s. Pulse sequences reported by Benn et al.⁴² and by Bax et al.⁴³ were used. Osmium-187 spectra of **IV** were obtained using approximately 20 mg of sample by applying a binomial suppression of the central phosphorus resonance.⁴⁴ Prior to Fourier transformation, the data were zero filled and multiplied by β functions in both dimensions. Chemical shifts are reported relative to OsO_4 in a field where the protons of TMS resonate at precisely 100 MHz ($\Xi = 2.282\ 343$ MHz).^{9,10} Osmium relaxation times T_1 were measured at the frequency of the ^{31}P nucleus by employing inverse detection methods recently developed in our group.⁴¹

Routine ^1H and ^{13}C NMR spectra were recorded at 300 K on a Bruker ARX-300 spectrometer and are referenced relative to TMS. ^{31}P NMR spectra were recorded on a Bruker AM-400 spectrometer and are referenced relative to 85% H_3PO_4 . For $^{13}\text{C}\{^1\text{H}\}$ shift assignments, the p-cymene carbon atoms have been labeled:



All reactions were performed in dry glassware under an inert atmosphere of nitrogen. Solvents were chemically dried

and distilled prior to use. The monomeric complexes **1**, **3-5**, **9**, **15**, and **29** and dimers $[\text{Os}(\text{p-cymene})\text{Cl}_2]_2$, $[\text{Os}(\text{C}_6\text{Me}_6)\text{Cl}_2]_2$, and $[\text{Os}(\text{C}_6\text{H}_6)\text{Cl}_2]_2$ were prepared by literature procedures.⁴⁵⁻⁴⁸ Complexes **13**, **16**, and **18** and osmium trichloride were generously donated by Dr. A. Hafner (Ciba-Geigy, Marly, Switzerland).

Os(p-cymene)Br₂PMe₃ (2). The dichloride **1** (140 mg, 0.3 mmol) and NaBr (300 mg, 3.0 mmol) were stirred in MeOH (10 mL) overnight at room temperature. The solution was evaporated, redissolved in CH_2Cl_2 (10 mL), and filtered (Celite), and the volume of solvent was reduced to 2–3 mL. Pentane (15 mL) was added to precipitate an orange powder, which was filtered out and washed with cold ether (5 mL). Yield: 150 mg (90%). Mp: 197–209 $^\circ\text{C}$. ^1H NMR (CDCl_3): p-cymene, δ 1.25 (d, $J = 6.9$ Hz, 6H, CHMe_2), 2.26 (s, 3H, Me), 2.87 (sept, $J = 6.9$ Hz, 1H, CHMe_2), 5.45 (m, 4H, $\text{MeC}_6\text{H}_4\text{-CHMe}_2$); PR_3 , δ 1.72 (d, $J = 10.4$ Hz, 9H, P–Me). $^{13}\text{C}\{^1\text{H}\}$ NMR (CDCl_3): p-cymene, δ 22.3 (s, C7), 18.9 (s, C1), 30.8 (s, C6), 99.1 and 87.9 (s, C2 and C5), 86.1 and 80.6 (s, C3 and C4); PR_3 , δ 16.8 (d, $J = 39.1$ Hz, P–Me). Anal. Calcd for $\text{C}_{13}\text{H}_{23}\text{Br}_2\text{OsP}$: C, 27.9; H, 4.11. Found: C, 28.3; H, 4.00.

Complexes **6-18** were similarly prepared by cleavage of $[\text{Os}(\text{p-cymene})\text{Cl}_2]_2$ using 2.2 equiv of PR_3 , of which a representative example is given for the $\text{P}(\text{OMe})_3$ -substituted complex **6**.

Os(p-cymene)Cl₂P(OMe)₃ (6). $[\text{Os}(\text{p-cymene})\text{Cl}_2]_2$ (150 mg, 0.2 mmol) and $\text{P}(\text{OMe})_3$ (0.5 mL, 0.45 mmol) were stirred in CH_2Cl_2 (10 mL) for 1 h at 40 $^\circ\text{C}$. The cooled solution was filtered (Celite) and the volume of solvent reduced to 2–3 mL. The product was purified by column chromatography using neutral grade (IV) alumina and diethyl ether as eluant. The solvent was evaporated, and the product was redissolved in CH_2Cl_2 (2 mL). Pentane (15 mL) was added to precipitate a yellow powder, which was filtered out and washed with cold ether (5 mL). Yield: 130 mg (70%). Mp: 149–151 $^\circ\text{C}$. ^1H NMR (CDCl_3): p-cymene, δ 1.27 (d, $J = 7.0$ Hz, 6H, CHMe_2), 2.28 (s, 3H, Me), 2.87 (sept, $J = 7.0$ Hz, 1H, CHMe_2), 5.66 (d, $J = 5.8$ Hz, 2H, $\text{MeC}_6\text{H}_4\text{CHMe}_2$), 5.12 (d, $J = 5.8$ Hz, 2H, $\text{MeC}_6\text{H}_4\text{CHMe}_2$); $\text{P}(\text{OR})_3$, δ 3.80 (d, $J = 11.2$ Hz, 9H, OMe). $^{13}\text{C}\{^1\text{H}\}$ NMR (CDCl_3): p-cymene, δ 22.1 (s, C7), 18.1 (s, C1), 30.1 (s, C6), 101.8 (d, $J = 3.2$ Hz, C2 or C5), 95.1 (d, $J = 2.2$ Hz, C2 or C5), 81.2 (d, $J = 4.8$ Hz, C3 or C4), 80.4 (d, $J = 5.7$ Hz, C3 or C4); $\text{P}(\text{OR})_3$, δ 53.6 (d, $J = 5.7$ Hz, P–OMe). Anal. Calcd for $\text{C}_{13}\text{H}_{23}\text{Cl}_2\text{O}_3\text{OsP}$: C, 30.1; H, 4.43. Found: C, 30.0; H, 4.31.

Os(p-cymene)Cl₂P(OEt)₃ (7): Yellow powder, yield 140 mg (66%). Mp: 89–91 $^\circ\text{C}$. ^1H NMR (CDCl_3): p-cymene, δ 1.27 (d, $J = 6.8$ Hz, 6H, CHMe_2), 2.27 (s, 3H, Me), 2.88 (sept, $J = 6.8$ Hz, 1H, CHMe_2), 5.63 (d, $J = 5.2$ Hz, 2H, $\text{MeC}_6\text{H}_4\text{CHMe}_2$), 5.48 (d, $J = 5.2$ Hz, 2H, $\text{MeC}_6\text{H}_4\text{CHMe}_2$); $\text{P}(\text{OR})_3$, δ 1.28 (t, $J = 6.8$ Hz, 9H, CH_3), 4.17 (m, $J = 6.8$ Hz, 6H, OCH_2). $^{13}\text{C}\{^1\text{H}\}$ NMR (CDCl_3): p-cymene, δ 22.2 (s, C7), 18.0 (s, C1), 30.1 (s, C6), 101.1 and 94.5 (s, C2 and C5), 81.0 (d, $J = 5.3$ Hz, C3 or C4), 80.3 (d, $J = 5.2$ Hz, C3 or C4); $\text{P}(\text{OR})_3$, δ 16.1 (d, $J = 6.0$ Hz, CH_3), 62.4 (d, $J = 6.0$ Hz, OCH_2). Anal. Calcd for $\text{C}_{16}\text{H}_{29}\text{Cl}_2\text{O}_3\text{OsP}$: C, 34.2; H, 5.17. Found: C, 34.5; H, 5.19.

Os(p-cymene)Cl₂P(OⁿBu)₃ (8): Orange powder, yield 145 mg (63%). Mp: 50–56 $^\circ\text{C}$. ^1H NMR (CDCl_3): p-cymene, δ 1.25 (d, $J = 6.9$ Hz, 6H, CHMe_2), 2.24 (s, 3H, Me), 2.85 (sept, $J = 6.9$ Hz, 1H, CHMe_2), 5.48 (d, $J = 5.7$ Hz, 2H, $\text{MeC}_6\text{H}_4\text{CHMe}_2$), 5.62 (d, $J = 5.7$ Hz, 2H, $\text{MeC}_6\text{H}_4\text{CHMe}_2$); $\text{P}(\text{OR})_3$, δ 0.94 (t, $J = 7.2$ Hz, 9H, CH_3), 4.08 (m, 6H, OCH_2), 1.41 (m, 6H, CH_2), 1.62 (m, 6H, CH_2). $^{13}\text{C}\{^1\text{H}\}$ NMR (CDCl_3): p-cymene, δ 22.2 (s, C7), 17.9 (s, C1), 30.1 (s, C6), 100.5 and 93.8 (s, C2 and C5), 80.9 (d, $J = 5.6$ Hz, C3 or C4), 80.6 (d, $J = 5.9$ Hz, C3 or

(45) Cabeza, J. A.; Maitlis, P. M. *J. Chem. Soc., Dalton Trans.* **1985**, 573.

(46) Werner, H.; Zenkert, K. *J. Organomet. Chem.* **1988**, 345, 151.

(47) Kiel, W. A.; Ball, R. G.; Graham, W. A. G. *J. Organomet. Chem.* **1990**, 383, 481.

(48) Arthur, T.; Stephenson, T. A. *J. Organomet. Chem.* **1981**, 208, 369.

(42) Benn, R.; Brevard, C. *J. Am. Chem. Soc.* **1986**, 108, 5622.

(43) Bax, A.; Griffey, R. H.; Hawkins, B. L. *J. Magn. Reson.* **1983**, 55, 301.

(44) Meier, E. J. M.; Koźmiński, W.; von Philipsborn, W. *Magn. Reson. Chem.* **1996**, 34, 89.

C4); P(OR)₃, δ 13.7 (s, CH₃), 66.1 (d, *J* = 6.6 Hz, OCH₂), 32.4 and 18.9 (s, CH₂). Anal. Calcd for C₂₂H₄₁Cl₂O₃OsP: C, 40.9; H, 6.36. Found: C, 40.7; H, 6.14.

Os(p-cymene)Cl₂P(OⁱPr)₃ (10): Orange powder, yield 190 mg (85%). Mp: 113–121 °C. ¹H NMR (CDCl₃): p-cymene, δ 1.26 (d, *J* = 6.9 Hz, 6H, CHMe₂), 2.23 (s, 3H, Me), 2.87 (sept, *J* = 6.9 Hz, 1H, CHMe₂), 5.61 (d, *J* = 5.7 Hz, 2H, MeC₆H₄-CHMe₂), 5.46 (d, *J* = 5.7 Hz, 2H, MeC₆H₄CHMe₂); P(OR)₃, δ 1.30 (d, *J* = 6.4 Hz, 18H, CH₃), 4.94 (m, *J* = 6.4 Hz, 3H, OCH). ¹³C{¹H} NMR (CDCl₃): p-cymene, δ 22.3 (s, C7), 17.7 (s, C1), 30.2 (s, C6), 100.0 and 95.3 (s, C2 and C5), 80.6 (d, *J* = 4.5 Hz, C3 or C4), 79.7 (d, *J* = 6.3 Hz, C3 or C4); P(OR)₃, δ 23.9 (d, *J* = 3.8 Hz, CH₃), 70.8 (d, *J* = 7.0 Hz, OCH). Anal. Calcd for C₁₉H₃₅Cl₂O₃OsP: C, 37.8; H, 5.80. Found: C, 37.9; H, 5.53.

Os(p-cymene)Cl₂PMe₂Ph (11): Orange powder, yield 180 mg (89%). Mp: 163–177 °C. ¹H NMR (CDCl₃): p-cymene, δ 1.12 (d, *J* = 7.0 Hz, 6H, CHMe₂), 1.96 (s, 3H, Me), 2.49 (sept, *J* = 7.0 Hz, 1H, CHMe₂), 5.34 (d, *J* = 5.1 Hz, 2H, MeC₆H₄-CHMe₂), 5.24 (d, *J* = 5.1 Hz, 2H, MeC₆H₄CHMe₂); PR₃, δ 1.85 (d, *J* = 10.7 Hz, 6H, P-Me), 7.45 (m, 3H, Ph), 7.07 (t, *J* = 8.5 Hz, 2H, Ph). ¹³C{¹H} NMR (CDCl₃): p-cymene, δ 21.8 (s, C7), 17.2 (s, C1), 29.7 (s, C6), 98.2 and 86.6 (s, C2 and C5), 80.2 (d, *J* = 3.8 Hz, C3 or C4), 80.1 (d, *J* = 4.5 Hz, C3 or C4); PR₃, δ 11.4 (d, *J* = 39.2 Hz, P-Me), 137.4 (d, *J* = 49.0 Hz, ipso C₆H₅), 129.7, 129.1, and 128.1 (s, Ph). Anal. Calcd for C₁₈H₂₅Cl₂-OsP: C, 40.3; H, 4.69. Found: C, 40.6; H, 4.82.

Os(p-cymene)Cl₂PPh₂Me (12): Orange-yellow powder, yield 200 mg (89%). Mp: 169–170 °C. ¹H NMR (CDCl₃): p-cymene, δ 0.92 (d, *J* = 7.0 Hz, 6H, CHMe₂), 1.98 (s, 3H, Me), 3.32 (sept, *J* = 7.0 Hz, 1H, CHMe₂), 5.45 (d, *J* = 5.7 Hz, 2H, MeC₆H₄CHMe₂), 5.39 (d, *J* = 5.7 Hz, 2H, MeC₆H₄CHMe₂); PR₃, δ 1.96 (d, *J* = 11.4 Hz, 3H, P-Me), 7.4–7.7 (m, 10H, Ph). ¹³C{¹H} NMR (CDCl₃): p-cymene, δ 21.7 (s, C7), 17.1 (s, C1), 29.6 (s, C6), 99.0 and 87.7 (s, C2 and C5), 80.7 and 77.9 (s, C3 and C4); PR₃, δ 11.1 (d, *J* = 39.6 Hz, P-Me), 134.7 (d, *J* = 52.0 Hz, ipso C₆H₅), 132.7, 130.3 and 128.0 (s, Ph). Anal. Calcd for C₂₃H₂₇Cl₂OsP: C, 46.4; H, 4.54. Found: C, 46.4; H, 4.6.

Os(p-cymene)Cl₂PPⁿBu₃ (14): Orange powder, yield 196 mg (87%). Mp: 176–179 °C. ¹H NMR (CDCl₃): p-cymene, δ 1.29 (d, *J* = 6.9 Hz, 6H, CHMe₂), 2.22 (s, 3H, Me), 2.77 (sept, *J* = 6.9 Hz, 1H, CHMe₂), 5.61 (d, *J* = 5.6 Hz, 2H, MeC₆H₄-CHMe₂), 5.40 (d, *J* = 5.6 Hz, 2H, MeC₆H₄CHMe₂); PR₃, δ 0.95 (d, *J* = 6.9 Hz, 9H, CH₃), 2.00 (m, 6H, P-CH₂), 1.40 (m, 12H, CH₂). ¹³C{¹H} NMR (CDCl₃): p-cymene, δ 22.3 (s, C7), 17.8 (s, C1), 30.3 (s, C6), 97.6 and 86.2 (s, C2 and C5), 80.1 (d, 3.1 Hz, C3 or C4), 76.6 (d, 6.5 Hz, C3 or C4); PR₃, δ 13.6 (s, CH₃), 23.7 (d, *J* = 32.9 Hz, P-CH₂), 25.1 (d, *J* = 12.7 Hz, CH₂), 24.2 (d, *J* = 3.1, CH₂). Anal. Calcd for C₂₂H₄₁Cl₂OsP: C, 44.2; H, 6.87. Found: C, 44.3; H, 6.67.

Os(p-cymene)Cl₂PPⁿPr₃ (17): Orange powder, yield 150 mg (71%). Mp: 142–146 °C. ¹H NMR (CDCl₃): p-cymene, δ 1.34 (d, *J* = 7.5 Hz, 6H, CHMe₂), 2.21 (s, 3H, Me), 2.83 (sept, *J* = 7.5 Hz, 1H, CHMe₂), 5.87 (d, *J* = 5.5 Hz, 2H, MeC₆H₄-CHMe₂), 5.78 (d, *J* = 5.5 Hz, 2H, MeC₆H₄CHMe₂); PR₃, δ 1.34 (dd, J(P,H) = 12.9 Hz, J(H,H) = 6.9 Hz, 18H, CH₃), 2.83 (m, 3H, P-CH). ¹³C{¹H} NMR (CDCl₃): p-cymene, δ 23.0 (s, C7), 17.9 (s, C1), 30.7 (s, C6), 97.5 and 87.2 (s, C2 and C5), 79.9 (d, 3.0 Hz, C3 or C4), 76.7 (d, 3.0 Hz, C3 or C4); PR₃, δ 20.1 (s, CH₃), 25.3 (d, *J* = 25.0 Hz, P-CH). Anal. Calcd for C₁₉H₃₅-Cl₂OsP: C, 41.1; H, 6.31. Found: C, 41.4; H, 6.17.

Complexes **19–24** were similarly prepared by halogen exchange of the corresponding dichloride complex of **III** using NaI, for which a representative example is given for the PMe₂Ph-substituted complex **19**.

Os(p-cymene)I₂PMe₂Ph (19). The dichloride **11** (50 mg, 0.09 mmol) and NaI (300 mg, 2.0 mmol) were stirred in MeOH (10 mL) overnight at room temperature. The solution was evaporated, redissolved in CH₂Cl₂ (10 mL), and filtered (Celite), and the volume of solvent was reduced to 2–3 mL. Pentane (15 mL) was added to precipitate a red powder, which was filtered out and washed with cold ether (5 mL). Yield:

44 mg (65%). Mp: 158–170 °C. ¹H NMR (CDCl₃): p-cymene, δ 1.11 (d, *J* = 6.9 Hz, 6H, CHMe₂), 2.10 (s, 3H, Me), 2.88 (sept, *J* = 6.9 Hz, 1H, CHMe₂), 5.27 (d, *J* = 5.7 Hz, 2H, MeC₆H₄-CHMe₂), 5.21 (d, *J* = 5.7 Hz, 2H, MeC₆H₄CHMe₂); PR₃, δ 2.24 (d, *J* = 10.4 Hz, 6H, P-Me), 7.40–7.28 (m, 5H, Ph). ¹³C{¹H} NMR (CDCl₃): p-cymene, δ 22.3 (s, C7), 19.4 (s, C1), 31.2 (s, C6), 102.4 and 87.7 (s, C2 and C5), 81.5 (d, 2.9 Hz, C3 or C4), 77.1 (d, 4.6 Hz, C3 or C4); PR₃, δ 18.7 (d, *J* = 42.7 Hz, P-Me), 139.1 (d, *J* = 45.5 Hz, ipso C₆H₅), 130.0 (s, Ph), 129.7 (d, *J* = 7.9 Hz, Ph), 128.3 (d, *J* = 9.3 Hz, Ph). Anal. Calcd for C₁₈H₂₅I₂OsP: C, 30.2; H, 3.49. Found: C, 30.2; H, 3.58. MS: *m/z* 718 [M⁺] (¹⁹²Os).

Os(p-cymene)I₂PⁿBu₃ (20): Red powder, yield 42 mg (60%). Mp: 156–164 °C. ¹H NMR (CDCl₃): p-cymene, δ 1.28 (d, *J* = 6.8 Hz, 6H, CHMe₂), 2.38 (s, 3H, Me), 3.13 (sept, *J* = 6.8 Hz, 1H, CHMe₂), 5.12 (m, 4H, MeC₆H₄CHMe₂); PR₃, δ 0.95 (t, *J* = 7.0 Hz, 9H, Me), 1.30–1.50 (m, 12H, CH₂), 2.23 (m, 6H, P-CH₂). ¹³C{¹H} NMR (CDCl₃): p-cymene, δ 22.5 (s, C7), 19.6 (s, C1), 31.5 (s, C6), 102.4 and 86.9 (s, C2 and C5), 80.9 and 76.2 (s, C3 or C4); PR₃, δ 13.7 (s, CH₃), 29.1 (d, *J* = 33.6 Hz, P-CH₂), 26.7 and 24.3 (s, CH₂). Anal. Calcd for C₂₂H₄₁I₂-OsP: C, 33.9; H, 5.26. Found: C, 33.6; H, 5.20. MS: *m/z* 782 [M⁺] (¹⁹²Os).

Os(p-cymene)I₂PPh₂Me (21): Red powder, yield 45 mg (64%). Mp: 183–193 °C. ¹H NMR (CDCl₃): p-cymene, δ 0.91 (d, *J* = 6.8 Hz, 6H, CHMe₂), 2.18 (s, 3H, Me), 2.81 (sept, *J* = 6.8 Hz, 1H, CHMe₂), 5.50 (d, *J* = 5.4 Hz, 2H, MeC₆H₄CHMe₂), 5.37 (d, *J* = 5.4 Hz, 2H, MeC₆H₄CHMe₂); PR₃, δ 2.57 (t, *J* = 10.0 Hz, 3H, P-Me), 7.41–7.37 (m, 10H, Ph). ¹³C{¹H} NMR (CDCl₃): p-cymene, δ 21.9 (s, C7), 18.6 (s, C1), 31.0 (s, C6), 102.7 and 88.7 (s, C2 and C5), 81.7 (s, C3 or C4), 78.3 (d, 4.7 Hz, C3 or C4); PR₃, δ 19.9 (d, *J* = 44.4 Hz, P-Me), 136.8 (d, *J* = 52.3 Hz, ipso C₆H₅), 133.3 (d, *J* = 9.0 Hz, Ph), 130.2 (s, Ph), 127.9 (d, *J* = 10.0 Hz, Ph). Anal. Calcd for C₂₃H₂₇I₂OsP: C, 35.5; H, 3.47. Found: C, 35.8; H, 3.53. MS: *m/z* 780 [M⁺] (¹⁹²Os).

Os(p-cymene)I₂PPh₃ (22): Red powder, yield 47 mg (62%). Mp: 220–223 °C. ¹H NMR (CDCl₃): p-cymene, δ 1.25 (d, *J* = 6.9 Hz, 6H, CHMe₂), 2.01 (s, 3H, Me), 3.33 (sept, *J* = 6.9 Hz, 1H, CHMe₂), 5.61 (d, *J* = 5.8 Hz, 2H, MeC₆H₄CHMe₂), 5.10 (d, *J* = 5.6 Hz, 2H, MeC₆H₄CHMe₂); PR₃, δ 7.40–7.75 (m, 15H, Ph). ¹³C{¹H} NMR (CDCl₃): p-cymene, δ 22.8 (s, C7), 18.6 (s, C1), 31.7 (s, C6), 105.2 and 91.4 (s, C2 and C5), 81.9 and 80.3 (s, C3 and C4); PR₃, δ 135.3 (d, *J* = 53.8 Hz, ipso C₆H₅), 135.8 (d, *J* = 9.0 Hz, Ph), 130.5 (s, Ph), 127.5 (d, *J* = 10.1 Hz, Ph). Anal. Calcd for C₂₈H₂₉I₂OsP: C, 40.0; H, 3.45. Found: C, 40.6; H, 3.52. MS: *m/z* 715 [M⁺ - I] (¹⁹²Os).

Os(p-cymene)I₂PⁱPr₃ (23): Red powder, yield 35 mg (53%). Mp: 151–163 °C. ¹H NMR (CDCl₃): p-cymene, δ 1.33 (d, *J* = 7.3 Hz, 6H, CHMe₂), 2.41 (s, 3H, Me), 3.17 (sept, *J* = 7.3 Hz, 1H, CHMe₂), 5.83 (m, 4H, MeC₆H₄CHMe₂); PR₃, δ 1.35 (dd, J(PH) = 13.1 Hz, J(H,H) = 7.4 Hz, 18H, CH₃), 3.01 (m, 3H, P-CH). ¹³C{¹H} NMR (CDCl₃): p-cymene, δ 23.1 (s, C7), 19.4 (s, C1), 31.6 (s, C6), 102.2 and 87.2 (s, C2 and C5), 81.6 and 76.1 (s, C3 and C4); PR₃, δ 21.1 (s, Me), 28.9 (d, *J* = 26.0 Hz, P-CH). Anal. Calcd for C₁₉H₃₅I₂OsP: C, 30.9; H, 4.74. Found: C, 30.9; H, 4.00. MS: *m/z* 613 [M⁺ - I] (¹⁹²Os).

Os(p-cymene)I₂PCy₃ (24): Red powder, yield 48 mg (62%). Mp: 143–151 °C. ¹H NMR (CDCl₃): p-cymene, δ 1.33 (d, *J* = 6.9 Hz, 6H, CHMe₂), 2.38 (s, 3H, Me), 3.19 (sept, *J* = 6.9 Hz, 1H, CHMe₂), 5.81 (m, 4H, *J* = 5.9 Hz, MeC₆H₄CHMe₂); PR₃, δ 2.26 (m, 3H, P-CH), 2.20 (m, 6H, CH₂), 1.81 (m, 12H, CH₂), 1.40 (m, 12H, CH₂). ¹³C{¹H} NMR (CDCl₃): p-cymene, δ 22.9 (s, C7), 19.3 (s, C1), 31.6 (s, C6), 102.4 and 87.0 (s, C2 and C5), 81.7 and 75.9 (s, C3 and C4); PR₃, δ 38.9 (d, *J* = 24 Hz, P-CH), 30.6 (s, CH₂), 27.3 (d, *J* = 9.6 Hz, CH₂), 26.5 (s, CH₂). No satisfactory microanalysis was obtained.

Os(p-cymene)HCIPMe₃ (25). Complex **1** (90 mg, 0.19 mmol) and Et₃N (0.5 mL, 0.5 mmol) were stirred at 80 °C in ethanol (20 mL) for 5 h. The cooled solution was filtered (Celite) and the volume of solvent reduced to 2–3 mL. The product was purified by column chromatography using neutral

grade (IV) alumina and diethyl ether as eluant, giving a yellow powder. Yield: 50 mg (60%). Mp: 121–123 °C. ^1H NMR (C_6D_6): p-cymene, δ 1.08 (d, $J = 6.7$ Hz, 3H, CHMe_2), 1.11 (d, $J = 6.7$ Hz, 3H, CHMe_2), 2.02 (s, 3H, Me), 2.13 (sept, $J = 6.7$ Hz, 1H, CHMe_2), 5.23 (d, 1H, $J = 5.2$ Hz, $\text{MeC}_6\text{H}_4\text{CHMe}_2$), 4.98 (d, 1H, $J = 5.2$ Hz, $\text{MeC}_6\text{H}_4\text{CHMe}_2$), 4.46 (d, 1H, $J = 5.6$ Hz, $\text{MeC}_6\text{H}_4\text{CHMe}_2$), 4.25 (d, 1H, $J = 5.6$ Hz, $\text{MeC}_6\text{H}_4\text{CHMe}_2$); PR_3 , δ 1.34 (d, $J = 10.0$ Hz, 9H, P–Me); $-\delta$ 8.63 (d, $J = 45.4$ Hz, 1H, Os–H). $^{13}\text{C}\{^1\text{H}\}$ NMR (C_6D_6): p-cymene, δ 25.1 and 23.2 (s, C7), 19.6 (s, C1), 32.4 (s, C6), 96.4 and 93.5 (s, C2 and C5), 78.8, 78.5, 78.6, 72.0 (s, C3 and C4); PR_3 , δ 20.8 (d, $J = 37.6$ Hz, P–Me). MS: m/z 437 [$\text{M}^+ - \text{H}$] (^{192}Os , ^{35}Cl), $\text{C}_{13}\text{H}_{24}\text{ClOsP}$. $\nu(\text{Os}-\text{H})$ (CH_2Cl_2): 2056 cm^{-1} .

Os(p-cymene)HCIPMe₂Ph (26). Complex 11 (90 mg, 0.17 mmol) and Et_3N (0.5 mL, 5.0 mmol) were stirred at 80 °C in ethanol (20 mL) for 5 h. The cooled solution was filtered (Celite) and the volume of solvent reduced to 2–3 mL. The product was purified by column chromatography using neutral grade (IV) alumina and diethyl ether as eluant, giving a yellow oil. Yield: 52 mg (62%). ^1H NMR (C_6D_6): p-cymene, δ 1.02 (d, $J = 6.8$ Hz, 3H, CHMe_2), 1.08 (d, $J = 6.8$ Hz, 3H, CHMe_2), 1.87 (s, 3H, Me), 2.00 (sept, $J = 6.8$ Hz, 1H, CHMe_2), 5.17 (d, 1H, $J = 5.6$ Hz, $\text{MeC}_6\text{H}_4\text{CHMe}_2$); 4.81 (d, 1H, $J = 5.3$ Hz, $\text{MeC}_6\text{H}_4\text{CHMe}_2$), 4.42 (d, 1H, $J = 5.6$ Hz, $\text{MeC}_6\text{H}_4\text{CHMe}_2$), 4.19 (d, 1H, $J = 5.3$ Hz, $\text{MeC}_6\text{H}_4\text{CHMe}_2$); PR_3 , δ 1.84 (d, $J = 10.3$ Hz, 3H, P–Me), 1.64 (d, $J = 10.0$ Hz, 3H, P–Me); 7.05–7.50 (m, 5H, Ph); $-\delta$ 8.59 (d, $J = 45.2$ Hz, 1H, Os–H). $^{13}\text{C}\{^1\text{H}\}$ NMR (C_6D_6): p-cymene, δ 24.9 and 23.1 (s, C7), 19.2 (s, C1), 31.9 (s, C6), 98.3 and 93.5 (s, C2 and C5), 80.2, 79.8, 79.0, 72.5 (s, C3 and C4); PR_3 , δ 21.2 (d, $J = 41.8$ Hz, P–Me), 17.6 (d, $J = 37.1$ Hz, P–Me), 141.4 (d, $J = 46.9$ Hz, ipso C_6H_5), 130.4 and 129.6 (s, Ph), remainder under solvent resonance. MS: m/z 500 [M^+] (^{192}Os , ^{35}Cl), $\text{C}_{18}\text{H}_{26}\text{ClOsP}$. $\nu(\text{Os}-\text{H})$ (CH_2Cl_2): 2022 cm^{-1} .

Os(p-cymene)HCIPⁿBu₃ (27). Complex 14 (90 mg, 0.15 mmol) and Et_3N (0.5 mL, 5.0 mmol) were stirred at 80 °C in ethanol (20 mL) for 5 h. The cooled solution was filtered (Celite) and the volume of solvent reduced to 2–3 mL. The product was purified by column chromatography using neutral grade (IV) alumina and diethyl ether as eluant, giving a yellow oil. Yield: 55 mg (65%). ^1H NMR (C_6D_6): p-cymene, δ 1.21 (d, $J = 7.3$ Hz, 3H, CHMe_2), 1.13 (d, $J = 6.7$ Hz, 3H, CHMe_2), 2.06 (s, 3H, Me), 2.14 (m, 1H, CHMe_2), 5.45 (d, 1H, $J = 5.7$ Hz, $\text{MeC}_6\text{H}_4\text{CHMe}_2$); 5.22 (d, 1H, $J = 5.1$ Hz, $\text{MeC}_6\text{H}_4\text{CHMe}_2$), 4.52 (d, 1H, $J = 5.7$ Hz, $\text{MeC}_6\text{H}_4\text{CHMe}_2$), 4.17 (d, 1H, $J = 5.1$ Hz, $\text{MeC}_6\text{H}_4\text{CHMe}_2$); PR_3 , δ 0.9 (t, $J = 7.1$ Hz, 9H, CH_3), 1.73 (m, 6H, P– CH_2); 1.32 (m, 12H, CH_2); $-\delta$ 8.61 (d, $J = 43.2$ Hz, 1H, Os–H). $^{13}\text{C}\{^1\text{H}\}$ NMR (C_6D_6): p-cymene, δ 24.9 and 22.0 (s, C7), 19.1 (s, C1), 32.5 (s, C6), 94.8 and 93.0 (s, C2 and C5), 81.1, 81.2, 78.6, 69.7 (s, C3 and C4); PR_3 , δ 14.5 (s, CH_3), 28.4 (d, $J = 33.2$ Hz, P– CH_2), 26.7 and 25.1 (s, CH_2). MS: m/z 564 [M^+] (^{192}Os , ^{35}Cl), $\text{C}_{22}\text{H}_{42}\text{ClOsP}$. $\nu(\text{Os}-\text{H})$ (CH_2Cl_2): 2060 cm^{-1} .

Os(p-cymene)HCIPPh₂Me (28). Complex 12 (90 mg, 0.15 mmol) and Et_3N (0.5 mL, 5.0 mmol) were stirred at 80 °C in ethanol (20 mL) for 5 h. The cooled solution was filtered (Celite) and the volume of solvent reduced to 2–3 mL. The product was purified by column chromatography using neutral grade (IV) alumina and diethyl ether as eluant, giving a yellow oil. Yield: 55 mg (65%). ^1H NMR (C_6D_6): p-cymene, δ 0.96 (d, $J = 6.8$ Hz, 3H, CHMe_2), 1.05 (d, $J = 7.2$ Hz, 3H, CHMe_2), 1.87 (s, 3H, Me), 1.81 (m, 1H, CHMe_2), 5.27 (d, 1H, $J = 5.6$ Hz, $\text{MeC}_6\text{H}_4\text{CHMe}_2$); 4.96 (d, 1H, $J = 5.2$ Hz, $\text{MeC}_6\text{H}_4\text{CHMe}_2$), 4.49 (d, 1H, $J = 5.6$ Hz, $\text{MeC}_6\text{H}_4\text{CHMe}_2$), 4.09 (d, 1H, $J = 5.2$ Hz, $\text{MeC}_6\text{H}_4\text{CHMe}_2$); PR_3 , δ 2.18 (d, $J = 9.8$ Hz, 3H, P–Me) 6.90–7.71 (m, 10H, Ph); $-\delta$ 8.40 (d, $J = 44.6$ Hz, 1H, Os–H). $^{13}\text{C}\{^1\text{H}\}$ NMR (C_6D_6): p-cymene, δ 24.9 and 22.9 (s, C7), 18.7 (s, C1), 31.5 (s, C6), 98.4 and 94.5 (s, C2 and C5), 81.4 (s, C3 or C4), 81.1 (d, $J = 5.3$ Hz, C3 or C4), 79.2 (s, $J = 6.0$ Hz, C3 or C4), 72.5 (s, C3 or C4); PR_3 , δ 20.3 (d, $J = 41.5$ Hz, P–Me), 140.7 (d, $J = 53.6$ Hz, ipso C_6H_5), 137.9 (d, $J = 47.2$ Hz, ipso C_6H_5), 133.1, 132.5, 130.1 and 129.6 (s, C_6H_5), remainder under

solvent resonance. MS: m/z 562 [M^+] (^{192}Os , ^{35}Cl), $\text{C}_{23}\text{H}_{28}\text{ClOsP}$. $\nu(\text{Os}-\text{H})$ (CH_2Cl_2): 2059 cm^{-1} .

Os(p-cymene)HCIPⁿPr₃ (30). Complex 17 (100 mg, 0.18 mmol) and Et_3N (0.5 mL, 0.5 mmol) were stirred at 80 °C in ethanol (20 mL) for 10 min. The cooled solution was filtered (Celite) and the volume of solvent reduced to 2–3 mL. The product was purified by column chromatography using neutral grade (IV) alumina and diethyl ether as eluant, giving a yellow oil. Yield: 84 mg (90%). ^1H NMR (C_6D_6): p-cymene, δ 1.99 (s, 3H, Me), 2.13 (sept, $J = 7.0$ Hz, 1H, CHMe_2), 5.61 (d, 1H, $J = 5.8$ Hz, $\text{MeC}_6\text{H}_4\text{CHMe}_2$); 5.50 (d, 1H, $J = 5.3$ Hz, $\text{MeC}_6\text{H}_4\text{CHMe}_2$), 4.41 (d, 1H, $J = 5.8$ Hz, $\text{MeC}_6\text{H}_4\text{CHMe}_2$), 4.19 (d, 1H, $J = 5.8$ Hz, $\text{MeC}_6\text{H}_4\text{CHMe}_2$), CHMe_2 under P^iPr_3 resonance; PR_3 , δ 1.04–1.23 (m, 24H, CHMe_2 and P– CHMe_2), 2.25 (m, 3H, P–CH); $-\delta$ 8.61 (d, $J = 41.5$ Hz, 1H, Os–H). $^{13}\text{C}\{^1\text{H}\}$ NMR (C_6D_6): p-cymene, δ 21.6 and 22.1 (s, C7), 18.9 (s, C1), 30.2 (s, C6), 95.8 and 91.0 (s, C2 and C5), 82.5, 81.0, 78.3 and 70.2 (s, C3 and C4); PR_3 , δ 19.9 (d, $J = 12.4$ Hz, Me), 27.0 (d, $J = 51.9$ Hz, P–CH). MS: m/z 522 [M^+] (^{192}Os , ^{35}Cl), $\text{C}_{19}\text{H}_{36}\text{ClOsP}$. $\nu(\text{Os}-\text{H})$ (CH_2Cl_2): 2084 cm^{-1} .

Os(p-cymene)HCIPCy₃ (31). Complex 18 (100 mg, 0.15 mmol) and Et_3N (0.5 mL, 5.0 mmol) were stirred at room temperature in ethanol (20 mL) for 10 min. The cooled solution was filtered (Celite) and the volume of solvent reduced to 2–3 mL. The product was purified by column chromatography using neutral grade (IV) alumina and diethyl ether as eluant, giving a yellow powder. Yield: 50 mg (53%). Mp: 153–159 °C. ^1H NMR (C_6D_6): p-cymene, δ 1.16 (d, $J = 6.9$ Hz, 3H, CHMe_2), 1.25 (d, $J = 6.9$ Hz, 3H, CHMe_2), 2.02 (s, 3H, Me), CHMe_2 under PCy_3 resonance, 5.68 (d, 1H, $J = 5.4$ Hz, $\text{MeC}_6\text{H}_4\text{CHMe}_2$); 5.61 (d, 1H, $J = 5.0$ Hz, $\text{MeC}_6\text{H}_4\text{CHMe}_2$), 4.40 (d, 1H, $J = 5.4$ Hz, $\text{MeC}_6\text{H}_4\text{CHMe}_2$), 4.26 (d, 1H, $J = 5.0$ Hz, $\text{MeC}_6\text{H}_4\text{CHMe}_2$); PR_3 , δ 2.21 (m, 3H, P–CH), 2.14 (m, 6H, CH_2); 1.95 (m, 4H, CH_2); 1.76 (m, 6H, CH_2); 1.54 (m, 12H, CH_2); $-\delta$ 8.45 (d, $J = 41.8$ Hz, 1H, Os–H). $^{13}\text{C}\{^1\text{H}\}$ NMR (C_6D_6): p-cymene, δ 25.6 and 21.4 (s, C7), 18.9 (s, C1), 31.7 (s, C6), 96.0 and 89.4 (s, C2 and C5), 82.7, 79.1, 78.3, 70.1 (s, C3 and C4); PR_3 , δ 37.0 (d, $J = 26.8$ Hz, P–CH), 30.1, 28.2, and 27.4 (CH_2). MS: m/z 641 [$\text{M}^+ - \text{H}$] (^{192}Os , ^{35}Cl), $\text{C}_{28}\text{H}_{48}\text{ClOsP}$. $\nu(\text{Os}-\text{H})$ (CH_2Cl_2): 2088 cm^{-1} .

Os(C₆H₆)Cl₂PMe₃ (32). $[\text{Os}(\text{C}_6\text{H}_6)\text{Cl}_2]_2$ (300 mg, 0.44 mmol) was stirred at 60 °C with PMe_3 (0.3 mL, 4 mmol) in toluene for 2 h. Additional PMe_3 (0.3 mL) was added and stirring continued for a further 2 h. The cooled solution was filtered (Celite) and washed with CD_2Cl_2 until the filtrate was clear. The solution was evaporated and redissolved in CH_2Cl_2 (5 mL), and pentane (20 mL) was added to obtain an orange precipitate, which was filtered off and washed with cold ether (5 mL). Yield: 210 mg (57%). Mp: decomposes at 220–230 °C. ^1H NMR (CDCl_3): δ 1.67 (d, 9H, $J = 11.1$ Hz, P–Me), 5.73 (s, 6H, C_6H_6). $^{13}\text{C}\{^1\text{H}\}$ NMR (CDCl_3): δ 15.0 (d, $J = 38.3$ Hz, P–Me), 78.6 (d, $J = 2.8$ Hz, C_6H_6). Anal. Calcd for $\text{C}_9\text{H}_{15}\text{Cl}_2\text{OsP}$: C, 26.0; H, 3.61. Found: C, 26.0; H, 3.95. MS: m/z 416 [M^+] (^{192}Os , ^{35}Cl).

$[\text{Os}(\text{C}_6\text{H}_5\text{Me})\text{Cl}_2]_2$. 2-Methylcyclohexa-1,4-diene ⁴⁹ (1.0 g, 100 mmol) and OsCl_3 (500 mg, 17 mmol) were stirred in ethanol (15 mL) for 3 days at 80 °C. The cooled solution was filtered (Celite) and washed with hot CDCl_3 , and the volume was reduced to 2–3 mL. Pentane (20 mL) was added to precipitate a yellow powder, which was filtered off and washed with cold ether (5 mL). Yield: 520 mg (87%). Mp: slowly decomposes above 170 °C. ^1H NMR (CDCl_3): δ 2.24 (s, 6H, Me), 6.05 (d, $J = 5.0$ Hz, 4H, CH), 6.21 (t, 2H, $J = 4.8$ Hz, CH), 6.28 (m, 4H, CH). ^{13}C DEPT NMR (CDCl_3): δ 19.7 (s, Me), 78.8, 72.2 and 70.8 (s, CH) (quaternary C not visible). Anal. Calcd for $\text{C}_{14}\text{H}_{16}\text{Cl}_2\text{Os}_2$: C, 23.8; H, 2.27. Found: C, 24.8; H, 2.93. MS: m/z 354 [$\text{M}^+/2$] (^{192}Os , ^{35}Cl).

(49) Krapcho, A. P.; Bothner-By, A. A. *J. Am. Chem. Soc.* **1959**, *81*, 3658.

(50) Johnson, C. K. *ORTEP II*; Report ORNL-5138; Oak Ridge National Laboratory: Oak Ridge, TN, 1976.

Os(C₆H₅Me)Cl₂PMe₃ (33). [Os(C₆H₅Me)Cl₂]₂ (150 mg, 0.2 mmol) and P(Me)₃ (0.2 mL, 2.6 mmol) were stirred in CH₂Cl₂ (15 mL) for 1 h at 40 °C. The cooled solution was filtered (Celite) and the volume reduced to 2–3 mL. Pentane (15 mL) was added to precipitate a yellow powder, which was filtered off and washed with cold ether (5 mL). Yield: 133 mg (73%). Mp: 209–215 °C. ¹H NMR (CDCl₃): δ 2.28 (s, Me), 5.67 (m, 2H, CH), 5.47 (m, 2H, CH), 5.42 (t, 1H, CH), 1.68 (d, *J* = 10.5 Hz, 9H, PMe₃). ¹³C{¹H} NMR (CDCl₃): δ 18.5 (s, 3H, Me), 15.4 (d, *J* = 38.2 Hz, PMe₃), 99.9 (s, quaternary), 78.7, 77.9, and 69.6 (s, CH). Anal. Calcd for C₁₀H₁₇Cl₂OsP: C, 28.0; H, 3.96. Found: C, 28.3; H, 3.57.

[Os(C₆H₅Et)Cl₂]₂. 2-Ethylcyclohexa-1,4-diene⁴⁹ (1.0 g, 100 mmol) and OsCl₃ (500 mg, 17 mmol) were stirred in ethanol (15 mL) for 3 days at 80 °C. The cooled solvent was filtered (Celite) and washed with hot CDCl₃, and the volume of solvent was reduced to 2–3 mL. Pentane (20 mL) was added to precipitate a yellow powder which was filtered off and washed with cold ether (5 mL). Yield: 560 mg (90%). Mp: decomposes 200–225 °C. ¹H NMR (CDCl₃): δ 1.29 (t, *J* = 7.4 Hz, 6H, CH₃), 2.55 (q, *J* = 7.4 Hz, 4H, CH₂), 6.08 (d, *J* = 4.4 Hz, 4H, CH), 6.20 (t, *J* = 3.9 Hz), 2H, CH), 6.28 (m, 4H, CH). ¹³C{¹H} NMR (CDCl₃): δ 14.0 (s, CH₃), 27.0 (s, CH₂), 94.2 (s, quaternary), 76.5, 71.7, and 71.4 (s, CH). Anal. Calcd for C₁₆H₂₀Cl₂Os₂: C, 26.2; H, 2.72. Found: C, 26.4; H, 3.13. MS: *m/z* 368 [M⁺/2] (¹⁹²Os, ³⁵Cl).

Os(C₆H₅Et)Cl₂PMe₃ (34). [Os(C₆H₅Et)Cl₂]₂ (200 mg, 0.27 mmol) and P(Me)₃ (0.2 mL, 2.6 mmol) were stirred in CH₂Cl₂ (15 mL) for 1 h at 40 °C. The cooled solution was filtered (Celite) and the volume reduced to 2–3 mL. Pentane (15 mL) was added to precipitate a yellow powder, which was filtered off and washed with cold ether (5 mL). Yield: 205 mg (84%). Mp: 176–179 °C. ¹H NMR (CDCl₃): δ 1.31 (t, *J* = 7.4 Hz, 3H, CH₃), 2.57 (q, *J* = 7.4 Hz, 2H, CH₂), 5.67 (m, 2H, CH), 5.52 (m, 2H, CH), 5.31 (t, *J* = 5.3 Hz, 1H, CH), 1.66 (d, *J* = 10.7 Hz, 9H, PMe₃). ¹³C{¹H} NMR (CDCl₃): δ 13.9 (s, CH₃), 15.7 (s, CH₂), 15.4 (d, *J* = 38.4 Hz, PMe₃), 103.6 (s, quaternary), 78.5, 77.5, and 70.3 (s, CH). Anal. Calcd for C₁₁H₁₉Cl₂OsP: C, 29.8; H, 4.29. Found: C, 29.8; H, 3.99.

[Os(C₆H₅ⁱPr)Cl₂]₂. 2-Isopropylcyclohexa-1,4-diene⁴⁹ (1.2 g, 100 mmol) and OsCl₃ (500 mg, 17 mmol) were stirred in ethanol (15 mL) for 3 days at 80 °C. The cooled solvent was filtered (Celite) and washed with hot CDCl₃, and the volume of solvent was reduced to 2–3 mL. Pentane (20 mL) was added to precipitate a yellow powder which was filtered off and washed with cold ether (5 mL). Yield: 460 mg (72%). Mp: slowly decomposes above 170 °C. ¹H NMR (CDCl₃): δ 0.31 (s, *J* = 6.2, 12H, CHMe₂), 2.82 (sept, *J* = 6.2, 2H, CHMe₂), 1.19 (m, 6H, CH), 5.46 (m, 4H, CH). ¹³C{¹H} NMR (CDCl₃): δ 22.2 (s, CH₃), 31.5 (s, CH), 69.3 (s, quaternary), 75.0, 73.0, and 71.8 (s, CH). Anal. Calcd for C₁₈H₂₄Cl₂Os₂: C, 28.4; H, 3.15. Found: C, 28.8; H, 2.85. MS: *m/z* 382 [M⁺/2] (¹⁹²Os, ³⁵Cl).

Os(C₆H₅ⁱPr)Cl₂PMe₃ (35). [Os(C₆H₅ⁱPr)Cl₂]₂ (200 mg, 0.26 mmol) and P(Me)₃ (0.2 mL, 2.6 mmol) were stirred in CH₂Cl₂ (15 mL) for 1 h at 40 °C. The cooled solution was filtered (Celite) and the volume reduced to 2–3 mL. Pentane (15 mL) was added to precipitate a yellow powder, which was filtered out and washed with cold ether (5 mL). Yield: 220 mg (92%). Mp: decomposes 180–195 °C. ¹H NMR (CDCl₃): δ 1.32 (s, *J* = 6.8, 6H, CHMe₂), 2.90 (sept, *J* = 6.8, 1H, CHMe₂), 5.59 (m, 4H, CH), 5.46 (t, *J* = 5.3 Hz, 1H, CH), 1.66 (d, *J* = 10.6 Hz, 9H, PMe₃). ¹³C{¹H} NMR (CDCl₃): δ 22.0 (s, CH₃), 30.6 (s, CH), 15.2 (d, *J* = 38.0 Hz, PMe₃), 107.7 (s, quaternary), 77.3, 77.0, and 70.3 (s, CH). Anal. Calcd for C₁₂H₂₁Cl₂OsP: C, 31.5; H, 4.60. Found: C, 31.4; H, 4.31.

[Os(C₆H₅^tBu)Cl₂]₂. 2-*tert*-Butylcyclohexa-1,4-diene⁴⁹ (1.3 g, 100 mmol) and OsCl₃ (500 mg, 17 mmol) were stirred in ethanol (15 mL) for 3 days at 80 °C. The cooled solvent was filtered (Celite) and washed with hot CDCl₃, and the volume was reduced to 2–3 mL. Pentane (20 mL) was added to precipitate a yellow powder, which was filtered off and washed

with cold ether (5 mL). Yield: 600 mg (90%). Mp: slowly decomposes above 180 °C. ¹H NMR (CDCl₃): δ 1.40 (s, 18H, CMe₃), 6.57 (d, *J* = 5.3 Hz, 4H, CH), 5.57 (m, 6H, CH). ¹³C{¹H} NMR (CDCl₃): δ 30.6 (s, CMe₃), 35.3 (s, CMe₃), 95.3 (s, quaternary), 77.6, 74.4, and 70.9 (s, CH). Anal. Calcd for C₂₀H₂₈Cl₂Os₂: C, 30.4; H, 3.54. Found: C, 30.5; H, 4.09. MS: *m/z* 396 [M⁺/2] (¹⁹²Os, ³⁵Cl).

Os(C₆H₅^tBu)Cl₂PMe₃ (36). [Os(C₆H₅^tBu)Cl₂]₂ (200 mg, 0.27 mmol) and P(Me)₃ (0.2 mL, 2.6 mmol) were stirred in CH₂Cl₂ (15 mL) for 1 h at 40 °C. The cooled solution was filtered (Celite) and the volume reduced to 2–3 mL. Pentane (15 mL) was added to precipitate a yellow powder, which was filtered out and washed with cold ether (5 mL). Yield: 210 mg (83%). Mp: decomposes at 180–200 °C. ¹H NMR (CDCl₃): δ 1.45 (s, 9H, CMe₃), 5.95 (d, *J* = 5.8 Hz, 2H, CH), 5.65 (m, 2H, CH), 5.46 (t, *J* = 5.2 Hz, 1H, CH), 1.63 (d, *J* = 10.6 Hz, 9H, P–Me). ¹³C{¹H} NMR (CDCl₃): δ 30.8 (s, CMe₃), 35.2 (s, CMe₃), 108.4 (d, *J* = 38.4 Hz, quaternary), 80.6 (d, *J* = 4.5 Hz, CH), 71.9 and 71.8 (s, CH). Anal. Calcd for C₁₂H₂₃Cl₂OsP: C, 33.1; H, 4.88. Found: C, 33.0; H, 4.68.

Os(C₆Me₆)Cl₂PMe₃ (37). [Os(C₆Me₆)Cl₂]₂ (200 mg, 0.24 mmol) and P(Me)₃ (0.2 mL, 2.6 mmol) were stirred in CH₂Cl₂ (15 mL) for 1 h at 40 °C. The cooled solution was filtered (Celite) and the volume reduced to 2–3 mL. Pentane (15 mL) was added to precipitate a yellow powder, which was filtered out and washed with cold ether (5 mL). Yield: 132 mg (62%). Mp: decomposes at 209–219 °C. ¹H NMR (CDCl₃): δ 2.08 (s, 18H, Me), 1.53 (d, *J* = 10.3 Hz, 9H, P–Me). ¹³C{¹H} NMR (CDCl₃): δ 16.0 (s, CMe), 87.3 (d, *J* = 3.7 Hz, CMe), 14.7 (d, *J* = 37.0, P–Me). Anal. Calcd for C₁₅H₂₇Cl₂OsP: C, 36.1; H, 5.41. Found: C, 35.6; H, 4.82. MS: *m/z* 500 [M⁺] (¹⁹²Os, ³⁵Cl).

X-ray Structure Determinations. The structures of **1**, **6**, **13**, and **15** were determined at 173 K. All measurements were made on a Rigaku AFC5R diffractometer using graphite-monochromated Mo K α radiation (λ = 0.710 69 Å) and a 12 kW rotating anode generator. For each compound, the intensities of three standard reflections were measured after every 150 reflections and remained stable throughout the data collection. The intensities were corrected for Lorentz and polarization effects. Semi-empirical absorption corrections, based on ψ -scans of several reflections, were applied to **1** and **13**.⁵¹ An analytical absorption correction was used for **6**,⁵² and an empirical absorption correction using the program DI-FABS⁵³ was used for **15** because other absorption correction methods produced unsatisfactory results. Equivalent reflections were merged. Data collection and refinement parameters are given in Table 6.

The structures were solved by Patterson methods using SHELXS86⁵⁴ and DIRDIF92,⁵⁵ which revealed the positions of the heavy atoms. All remaining non-hydrogen atoms were located in Fourier expansions of the Patterson solutions. The non-hydrogen atoms were refined anisotropically. The H atoms were fixed in geometrically calculated positions [$d(\text{C} - \text{H}) = 0.95$ Å], and they were assigned fixed isotropic temperature factors with a value of 1.2 U_{eq} of the parent C atom. The orientations of the methyl group H atoms were based on peaks located in difference electron density maps. Refinement of each structure was carried out on F using full-matrix least-squares procedures, which minimized the function $\sum w(|F_o| - |F_c|)^2$. The weighting scheme was based on counting statistics and included a factor to downweight the intense reflections. Plots of $\sum w(|F_o| - |F_c|)^2$ versus $|F_o|$, reflection order in data

(51) North, A. C. T.; Phillips, D. C.; Mathews, F. S. *Acta Crystallogr.* **1968**, *A24*, 351.

(52) De Meulenaer, J.; Tompa, H. *Acta Crystallogr.* **1965**, *19*, 1014.

(53) Walker, N.; Stuart, D. *Acta Crystallogr.* **1983**, *A39*, 158.

(54) Shelldrick, G. M. SHELXS-86. *Acta Crystallogr.* **1990**, *A46*, 467.

(55) Beurskens, P. T.; Admiraal, G.; Beurskens, G.; Bosman, W. P.; Garcia-Granda, S.; Smits, J. M. M.; Smykalla, C. *DIRDIF-92. The DIRDIF program system*; Technical Report of the Crystallography Laboratory; University of Nijmegen: Nijmegen, The Netherlands, 1992.

Table 6. Crystallographic Data for **1**, **6**, **13**, and **15**

	1	6	13	15
crystallized from	methanol	hexane/ethyl acetate	ethanol	CH ₂ Cl ₂
empirical formula	C ₁₃ H ₂₃ Cl ₂ OsP	C ₁₃ H ₂₃ Cl ₂ O ₃ OsP	C ₃₁ H ₃₅ Cl ₂ OsP	C ₂₈ H ₂₉ Cl ₂ OsP·CH ₂ Cl ₂
fw	471.40	519.40	699.70	742.55
cryst color, habit	orange, thin prism	orange, needle	orange, prism	orange, irregular prism
cryst dimens, mm	0.08 × 0.25 × 0.43	0.10 × 0.21 × 0.39	0.15 × 0.25 × 0.30	0.38 × 0.38 × 0.43
temp, K	173(1)	173(1)	173(1)	173(1)
cryst system	monoclinic	monoclinic	triclinic	triclinic
space group	<i>P</i> 2 ₁ / <i>n</i>	<i>P</i> 2 ₁ / <i>c</i>	<i>P</i> $\bar{1}$	<i>P</i> $\bar{1}$
Z	8	4	2	2
reflcs for cell determ	25	25	25	25
2θ range for cell determ, deg	39–40	39–40	39–40	39–40
a, Å	10.269(6)	13.329(2)	10.381(1)	12.625(2)
b, Å	27.168(7)	7.286(2)	14.610(1)	13.509(2)
c, Å	13.002(4)	17.480(2)	9.277(1)	9.361(2)
α, deg	90	90	96.860(9)	109.38(1)
β, deg	112.37(3)	91.48(1)	97.01(1)	102.27(2)
γ, deg	90	90	88.631(8)	99.67(1)
V, Å ³	3354(2)	1697.1(5)	1386.4(3)	1421.4(5)
F(000)	1808	1000	692	728
D _x , g cm ⁻³	1.867	2.033	1.676	1.735
μ(Mo Kα), mm ⁻¹	7.991	7.921	4.865	4.932
scan type	ω	ω/2θ	ω/2θ	ω/2θ
2θ(max), deg	55	60	60	60
min and max transm factors	0.449, 1.000	0.096, 0.378	0.479, 1.000	0.818, 1.098
tot. reflcs measd	8276 (+ <i>h</i> , + <i>k</i> , ± <i>l</i>)	5515 (+ <i>h</i> , + <i>k</i> , ± <i>l</i>)	8494 (+ <i>h</i> , ± <i>k</i> , ± <i>l</i>)	8592 (+ <i>h</i> , ± <i>k</i> , ± <i>l</i>)
sym indepdt reflcs	7679	4949	8088	8249
R _{merge}	0.020	0.054	0.017	0.021
reflcs used [<i>I</i> > 2σ(<i>I</i>)]	6097	3665	7341	7327
params refined	307	181	316	316
R	0.0296	0.0335	0.0233	0.0285
R _w	0.0260	0.0288	0.0228	0.0325
weights: <i>p</i> in <i>w</i> = [σ ² (<i>F</i> _o) + (<i>pF</i> _o) ²] ⁻¹	0.005	0.005	0.005	0.01
goodness of fit	1.364	1.330	1.367	1.549
final Δ _{max} /σ	0.0007	0.0008	0.002	0.001
max and min Δρ, e Å ⁻³	1.48, -0.89	1.26, -1.03	1.72, -1.13	1.29, -1.25

Downloaded by CARLI CONSORTIUM on June 30, 2009
 http://pubs.acs.org
 DOI: 10.1021/ol96053i

collection, (sin θ)/λ, and various classes of indices showed no unusual trends. Corrections for secondary extinction were not applied.

Neutral atom scattering factors for non-hydrogen atoms were taken from Maslen, Fox, and O'Keefe,^{56a} and the scattering factors for H atoms were taken from Stewart, Davidson, and Simpson.⁵⁷ Anomalous dispersion effects were included in *F*_c;⁵⁸ the values for *f*' and *f*" were those of Creagh and McAuley.^{56b} All calculations were performed using the TEXSAN crystallographic software package.⁵⁹

The structure of **1** has two molecules in the asymmetric unit; however, there are no major differences in their conformation other than a small rotation of the PMe₃ group. Some of the terminal methyl groups, especially in molecule A, are undergoing strong thermal motion (rotation about the C(1)–C(7)

bond) or are slightly disordered. However, no attempt was made to resolve any potential disorder. As a result, the C(7)–C(8) and C(7)–C(9) bond lengths appear to be shorter than they probably are. The crystals of **15** contain molecules of CH₂Cl₂ in a ratio of 1:1 with the osmium complex. The residual electron density of between 1.2 and 1.7 e Å⁻³ in each structure was located near the Os atoms and near the Cl atoms of the solvent molecule in **15**. The latter peaks might be due to slight disorder of the solvent molecule.

Acknowledgment. We thank the Swiss National Science Foundation and Dr. Helmut Legerlotz-Stiftung for financial support and Dr. A. Hafner (Ciba-Geigy, Marly, Switzerland) for providing stimulating discussions.

Supporting Information Available: Listings of fractional atomic coordinates and equivalent isotropic temperature factors, interatomic distances, bond angles, torsion angles, anisotropic temperature factors, and hydrogen atom coordinates for compounds **1**, **6**, **13**, and **15** (24 pages). Ordering information is given on any current masthead page.

OM960053I

(56) *International Tables for Crystallography*; Wilson, A. J. C., Ed.; Kluwer Academic Publishers: Dordrecht, The Netherlands, 1992; Vol. C: (a) Maslen, E. N.; Fox, A. G.; O'Keefe, M. A. Table 6.1.1.1, pp 477–486; (b) Creagh, D. C.; McAuley, W. J. Table 4.2.6.8, pp 219–222.

(57) Stewart, R. F.; Davidson, E. R.; Simpson, W. T. *J. Chem. Phys.* **1965**, *42*, 3175.

(58) Ibers, J. A.; Hamilton, W. C. *Acta Crystallogr.* **1964**, *17*, 781.

(59) TEXSAN. *Single Crystal Structure Analysis Software*, Version 5.0; Molecular Structure Corp.: The Woodlands, TX, 1989.